

Climate adaptation under uncertainty

A novel decision scaling approach to assess
climate vulnerability in the Waterberg
Biosphere Reserve, South Africa

Charlotte van Strien

Climate adaptation under uncertainty

A novel decision scaling approach to assess climate vulnerability in the Waterberg Biosphere Reserve, South Africa

by

C.F. (Charlotte) van Strien

to obtain the degree of Master of Science

at the Delft University of Technology,

to be defended publicly on Monday July 4 2022.

Student number: 4401093
Date: 27 June 2022
Thesis committee: Dr. M.M. Rutten, TU Delft, chair
Dr. R.J. van der Ent, TU Delft
Dr. M.U. Taner, Deltares



Onzekere tijden

Gelukkig wist ik eigenlijk
Nog nooit iets zeker

- Loesje

Preface

When I started one year ago with my thesis internship at Deltares on dynamic climate adaptation pathways, I could not have imagined that the result would be as it lies before you. The process of conducting this thesis appeared to be a dynamic adaptation pathway in itself! During the journey, I learned how to apply the knowledge I gained during the master's track Watermanagement at the faculty of Civil Engineering in Delft. Also, I discovered what topics energize me, and what topics fit me less. In the end, I am very pleased that I could combine my fascination for international climate adaptation, global climate models and projections, and hydrology into one study. Hopefully, reading this thesis also arouses your interest and teaches you a bit about the complexity of climate adaptation projects.

I am very grateful to everyone near me that gave me the room to explore this path. First of all, a special thanks to my supervisors. Martine, your sympathetic ear, safety, sharp questions, and time helped me structure my thoughts and make decisions along the way. Also Umit, thanks a lot for introducing me to Deltares, weather generators, and decision scaling. It was a pleasure to together discover about doing an internship at Deltares and connecting wflow with weather generators. Ruud, your critical feedback and new perspective along the way helped me look at my research with fresh eyes.

Next, thanks to all my colleagues at Deltares for inspiring me with your work. Laurene, I was happy to work with you again after three years and that you were always available for questions about wflow-sbm models. Sadie, thank you for sharing your expertise in South Africa. Valesca, for your contribution to implementing environmental flows and Ad and Frederieke, thanks for having me in the projects.

Last but not least, I would like to thank all my friends and family who were there for me over the past year. You were there to share my enthusiasm with but also my frustrations. The, sometimes forced, relaxation moments with you were indispensable in this period.

Charlotte van Strien
Rotterdam, 4 July 2022

Abstract

Managing water resources for the future is challenging, given the wide range of climatic and hydrological uncertainty. To support decision makers in formulating robust adaptation plans and finding their way through the broad range of available climate data and models, decision scaling was introduced: an approach for bottom-up climate vulnerability assessments, informed by Global Climate Models (GCMs). This study aims to improve decision scaling as developed by Brown et al. (2012) by introducing three recent advances in climate adaptation and uncertainty science.

First, the concept of environmental flows (eflows) was adopted to represent the local ecology and variable hydrology with a broad range of indicators for evaluating the impact of climate change. Second, the GCM weighting strategy of Knutti et al. (2017) was applied to account for model performance and interdependency when estimating the plausibility of future climate conditions. Lastly, climate stress testing was not only done for annual average climate changes, but also for a prolonged dry season to represent the interannually variable character of climate change. The potential application of the novel decision scaling approach was illustrated through a case study of the Mokolo River. This river is situated in the South African Waterberg Biosphere Reserve, which faces competing water demands from tourism, industry, agriculture, and ecology under a changing climate.

It was found that the additions contribute to decision scaling, as eflows indicators introduced the climate impact on multiple flow components, which provides extra information on the climate vulnerability of the river during different flow conditions. In Waterberg, low and average flow conditions were found similarly sensitive to climate change. Moreover, GCM weighting increased the range of temperature uncertainty and showed high weights for both wet and dry GCM projections, which emphasizes the need for robust climate adaptation in Waterberg. Next, the additional stress test showed that prolonging the dry season by one month influences flows throughout the following year, especially in the posterior months. In this way, understanding the impact of plausible characteristics of future climate was improved.

Finally, this study revealed that local activities, such as groundwater extractions and land use changes, and available knowledge challenges the application of decision scaling to a real case study as it requires models and quantification of indicators. Therefore, carefully matching models, performance indicators, local concerns and knowledge are required for formulating climate adaptation strategies with decision scaling.

Table of Contents

1	Introduction	1
2	Study Area	3
3	Materials & Methods	4
3.1	Hydrological Model	4
3.2	Data	6
3.2.a	Historical climate data	6
3.2.b	Historical streamflow data	6
3.2.c	Climate model projections	6
3.3	Historical climate trends & future projections	7
3.4	Environmental flows	7
3.4.a	Existing environmental flow indicators	7
3.4.b	Selection of performance indicators	10
3.4.c	Compliance to the concept of environmental flows	10
3.5	Global Climate Model Weighting	10
3.6	Climate Stress Testing	11
3.6.a	Stochastic Weather Generator	11
3.6.b	Climate stress test for average annual mean changes	12
3.6.c	Climate stress test for an prolonged dry season	12
3.6.d	Performance thresholds and risk	12
4	Results	14
4.1	Historical climate trends & future projections	14
4.2	Environmental Flows	15
4.2.a	Local stakeholder discussion	15
4.2.b	Selection of performance indicators	16
4.2.c	Compliance to the concept of environmental flows	16
4.3	Global Climate Model Weighting	16
4.4	Climate Stress Testing	20
4.4.a	Climate stress test for average annual mean changes	20
4.4.b	Climate stress test for an prolonged dry season	21
4.4.c	Performance thresholds and risk	21
5	Discussion	23
5.1	Data	23

5.2 Hydrological model	23
5.3 Environmental flows	24
5.4 Global Climate Model Weighting	26
5.5 Climate stress test	26
6 Conclusion	28
References	30
Supplementary Material	37
A Hydrological Model	37
B ERA5 precipitation scaling	39
C Global Climate Models	41
D GCM projections	42
E Climate stress test	44
F Global Climate Model Weighting	45

1 | Introduction

Global climate change impacts river flow regimes substantially (Arnell & Gosling, 2013), leading to floods, drinking water shortages, crop failure, and ecological loss (Mendoza et al., 2018). This asks water managers to focus more and more on climate adaptation. Planning for climate adaptation is however not that straightforward, as there are many uncertainties in how future climate will evolve. These uncertainties mainly originate from insufficient knowledge of natural variability, natural and anthropogenic forcing, model uncertainty and inadequacy, and from a relatively short observation time (Stainforth et al., 2007; Herman et al., 2020). This type of planning is often referred to as “decision making under deep uncertainty”: a situation in which the analysts do not know, or the stakeholders cannot agree on how to capture the system in a model, the probability distributions of the associated parameters, and the desirability of alternative outcomes (Lempert et al., 2003).

Typically, global climate model (GCM) projections are used in climate adaptation to inform on what future climate might look like and the corresponding range of uncertainty. However, regional water management assesses climate impact on a finer level by developing hydrological models that do not match the coarse spatial and temporal resolutions of GCMs which are generally more than 100 km and in monthly timesteps (Whateley et al., 2016). For that, dynamical and statistical downscaling techniques using high-resolution regional models and statistical relationships between climate variables have been widely developed. However, as the GCMs do not capture subgrid scale features such as topography, clouds, and land use, local phenomena are missed (Chokkavarapu & Mandla, 2019). This causes a poor representation of climatic variability and the magnitude and duration of extremes (Rocheta et al., 2014; Fowler et al., 2007), which could lead to an underestimation of the severity of climate change in terms of interannual variability and monthly means (Murphy, 1998). Therefore, the possible range of future climates might not be fully explored, leading to the fact that GCM projections often only show the lower bound of the uncertainty range (Stainforth et al., 2007).

In reaction to the limitations of the top-down approach as described above, bottom-up approaches have been introduced. These first identify system performance thresholds independently from GCM projections and subsequently assess the performance response when exposed to a wide range of plausible climate changes that go beyond the bounds of GCM projections (Culley et al., 2016). One example of such a bottom-up climate risk assessment linking climate-informed vulnerability assessments was developed by Brown et al. (2012), named “decision scaling”. This is a three-step approach that begins with identifying, mapping and modelling local problems and corresponding performance indicators and thresholds together with stakeholders. Then, these indicators are stress tested against a wide range of climate conditions to better understand the system’s climate vulnerability. This is done by running a large set of stochastic timeseries simulated by a stochastic weather generator. Lastly, it is evaluated which climate conditions lead to acceptable or unacceptable system performance. The plausibility of these conditions is estimated based on information from GCMs. By not only relying on GCM information and by using stakeholder-determined performance indicators, decision scaling allows for transparency and well-informed discussions between scientists, planners, and stakeholders on what adaptation measures to take (Poff et al., 2015).

Recently, decision scaling has been adopted by various researchers (e.g. by Ray et al. (2020); Conway et al. (2019); Mendoza et al. (2018); Culley et al. (2016); Whateley et al. (2016); Poff et al. (2015); García et al. (2014)). These studies focus on issues around human-made infrastructure, such as water supply reliability, urban flooding, and water security. Only Poff et al. (2015) explored decision scaling in ecological issues, though emphasizing the impact of human-made infrastructures rather than climate change itself. Moreover, the studies demonstrate decision scaling in hypothetical or stylized case studies based on synthetic data and simplifying assumptions. Three of these simplifications have been identified by literature as points of improvement, where recent advances in climate adaptation might be of help. Those simplifications and potentially helpful techniques are as follows.

- In decision scaling, basin performance is commonly evaluated for time-independent performance indicators such as average annual flow. In applied cases to for example dam operation, flood control, and ecological protection, these static indicators might however not be sufficiently informative. Therefore, the concept of environmental flows is frequently used in watermanagement projects to formulate such dynamic and ecologically relevant indicators. Environmental flows (eflows) are defined as “the quantity, timing, and quality of water flows required to sustain freshwater and estuarine ecosystems and the human livelihoods and well-being that depend on these ecosystems” (Poff & Matthews, 2013). As eflows are intended to mimic the natural river flow dynamics (The Nature Conservancy, 2019), using eflow indicators in decision scaling would require a shift from testing one static variable towards testing multiple time-varying indicators (Poff, 2018). Likewise performance indicators in decision scaling, eflows should be determined by involving both stakeholders and scientists to develop science-based policies and management (Poff et al., 2003). Eflows application in decision scaling could therefore be beneficial for both concepts.
- When estimating climate risk plausibility, GCM projections are assumed to be equiprobable, independent, and distributed around reality in the estimation of climate risk plausibility. However, as models share codes and do not represent the locally observed climate equally well, these assumptions cannot be validated (Merrifield et al., 2020; Sperna Weiland et al., 2021; Knutti et al., 2017). To add more statistical reasoning behind the uncertainty range from GCM projections, weighting strategies have been developed. One strategy is ClimWIP (Climate model Weighting by Independence and Performance), which weighs each GCM based on how closely it resembles the observed climate, and on its similarity to other models (e.g. in Brunner et al. (2020); Knutti et al. (2017); Lorenz et al. (2018); Merrifield et al. (2020)). This method might provide additional information to risk estimation in climate adaptation projects.
- In decision scaling, basins are commonly climate stress tested under changes in annual mean temperature and precipitation (e.g. in Ray et al. (2020); Kim et al. (2018); Culley et al. (2016); Poff et al. (2015); Brown et al. (2012)). Climate change, however, is often found to express itself in a change in variability, magnitudes of local extremes, and the duration and timing of seasons (Masson-Delmotte et al., 2021). This natural variation, which is larger for precipitation than temperature, and larger for climate extremes than means (van den Hurk et al., 2014), is thus not considered in stress tests. Stochastic weather generators in decision scaling have the feature to adapt this variability and duration of climate events in weather timeseries. Employing this feature in climate stress tests could give broader information on the climate vulnerability of a region.

This study develops a novel approach to decision scaling, focusing on implementing the three hypotheses detailed in the enumeration above. To demonstrate the application in a real case study, the South African arid region of the Waterberg Biosphere Reserve which deals with drought problems is used. In contrast to previously demonstrated cases of decision scaling, Waterberg is a data scarce environment where the preservation of environmental quality is of high importance.

This thesis is organised as follows. The Waterberg Biosphere Reserve is further introduced in the next chapter regarding its geographical, climatic, ecological, and societal characteristics. Then, the methodology of this study is described by explaining the models, data, and methods for environmental flow indicators, GCM weighting and stress testing. Chapter 4 shows the resulting indicators that can be used as performance indicators, and how they fit into the concept of eflows. Also, this chapter presents the results of GCM weighting and stress testing Waterberg under annual- and intra-annual climate changes. The impact of the novel approach to decision scaling is subsequently discussed in Section 5. The thesis finishes with a conclusion on how the three methods contribute to decision scaling.

2 | Study Area

The Waterberg is a 14 000 km² upland area located in the Limpopo Province of South Africa, with the town of Vaalwater in its centre (see Figure 2.1). In 2001, UNESCO designated one-third of the area (6500 km²) as a Biosphere Reserve that, together with 86 other South African reserves and 701 reserves worldwide, serves as a learning place for sustainable development in the field of biodiversity and cultural diversity, economic development, and logistic support for research and education (UNESCO, 2021). The western and eastern parts of the Waterberg Biosphere Reserve (WBR) are hilly, rocky, and at around 1300 m high. The central part close to Vaalwater consists of sandy plains below 1300 m. A mountain range is situated on the southern and eastern sides.

The plateau is a hot and dry region with a big range in altitudes that lead to high slopes and sparse rainfall events that are very location dependent. The annual average rainfall is approximately 610 mm and it knows a relatively wet season from October to April, with the most precipitation occurring between December and February. During the dry season, there is almost no rainfall. Temperatures range between 14°C in July and 25°C in December. This climate pattern greatly influences the discharge of the four rivers flowing through the WBR: the Mokolo, Lephalale, Matlabas and Mogalakwena, all tributaries of the Limpopo River. The rivers function as an important source of water for the rest of the region in terms of biodiversity and economic activity. The latter is nowadays mainly focused on game farming and tourism, which is rapidly growing. Agriculture is also important in the region: large parts of the Mokolo and Lephalale rivers are surrounded by irrigation fields, and small dams are built for water regulation (see Figure 2.1). The Mokolo Dam (146 million m³) serves municipal and industrial water. The most important industry is mining (Lyon et al., 2017).

Currently, the competing water demands in the reserve, combined with increasing stresses from a changing climate, are causing problems with water availability and allocation, and the ability to sustainable management of water resources. This challenges the region to maintain its status as a biosphere reserve. For that, monitoring programs for ecology and climate are starting up in the understudied area (Government of South Africa, 2015). After all, the uncertain nature of climate effects, particularly concerning changing seasonality and uncertain future rainfall patterns, asks for a better understanding of the region's hydrological behaviour and climate vulnerability to reveal adaptation possibilities. Decision scaling could therefore provide relevant information.

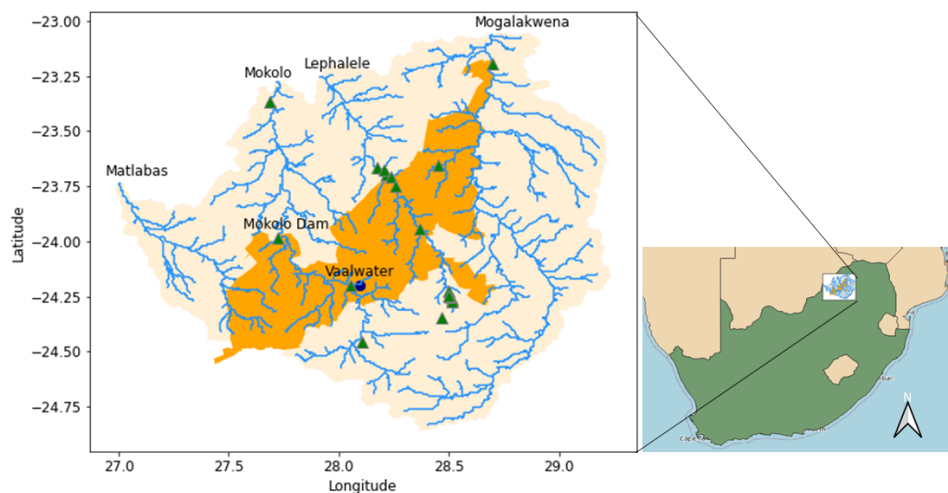


Figure 2.1 – Map of the four river catchments that flow through the Waterberg Biosphere Reserve (in orange), the town of Vaalwater, and the existing dams (green triangles). Dam locations are retrieved from Mulligan et al. (2020). The location of Waterberg within South Africa is indicated on the right.

3 | Materials & Methods

This chapter describes the data, models, and methods to apply and evaluate the decision scaling approach as proposed in Chapter 1. An overview of the workflow designed to implement the environmental flows concept, GCM weighting, and interannual variability in decision making can be found in Figure 3.4. Before explaining the implementation of these three suggestions in Sections 3.4 to 3.6, Section 3.3 presents how a historical and future climate analysis was done. This analysis forms the basis for further decisions in model- and climate stress test setup. Because of model performance and data availability, the methodology was performed for the Mokolo River catchment in the Waterberg region.

3.1. Hydrological Model

The hydrological conditions in the Mokolo River basin were modelled with a daily distributed wflow-sbm model (Schellekens et al., 2021). This conceptual bucket model simplifies the Richards equation by assuming that infiltration, vertical flow through the soil column, and capillary rise are gravity based. It makes use of the kinematic wave approach for lateral subsurface-, overland-, and river flow routing throughout the catchment. As flows are mainly controlled by topography, wflow-sbm parameters physical characteristics such as vegetation and soil properties, and thus have a clear physical meaning (Weerts et al., 2020). To derive these parameters, available pedotransfer functions from literature with upscaling rules from the Multiscale Parameter Regionalization technique from Samaniego et al. (2010) (both further explained in Imhoff et al. (2020)) are used by the model to convert spatial data maps to model parameter maps. For this, land use maps of VITO (Buchhorn et al., 2020) and the ISRIC soil database (Poggio et al., 2021) were used.

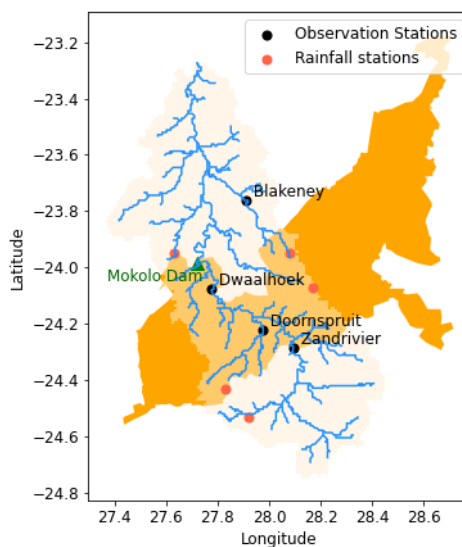


Figure 3.1 – Map of the wflow-sbm model extent for the Mokolo River basin (light orange). The Waterberg Biosphere Reserve is shown in bright orange. Locations and names of the Mokolo Dam and discharge- and rainfall observation stations are indicated.

The model was developed at a resolution of approximately 1km x 1km at the equator and the modelled area extent is defined between 27.4° and 28.4°E, and -23.3° and -24.7°S. This area covers more than 19 000 km², from which the central part belongs to the biosphere area (see Figure 3.1). To include upstream influences, the whole catchment extent was modelled. The required daily spatially distributed precipitation and temperature forcing data (see Section 3.2.a) were reprojected to WorldClim 2.1 high

resolution monthly climatology and meteorology data (approximately 0.04°) (Fick & Hijmans, 2017). The Mokolo Dam (146 million m^3) was included in the model as a reservoir. The capacity of the three other dams in the Mokolo (see Figure 2.1) is 2% of the annual streamflow and was assumed to be negligible. Other groundwater or river extractions were also not included.

Given that wflow-sbm is mainly sensitive to the rooting depth and the lateral hydraulic conductivity (Imhoff et al., 2020), calibration to observed streamflow data was done by tuning two parameters: the saturated horizontal conductivity, and the decrease of vertical saturated conductivity over the soil depth. Model output from ten combinations of parameter values was compared regarding their representation of the environmental flow indicators that are also used in the climate stress tests (see Section 3.6.d). These are listed and explained in Table 3.3. None of the model configurations was able to represent both dry- and wet-seasonal flows well. Eventually, the set of model parameters that lead to the lowest root-mean-square error between modelled and observed environmental flows was selected for this study. The errors and Nash Sutcliffe efficiencies (Nash & Sutcliffe, 1970) for the selected model can be found in Table 3.1. Supplementary Material A provides these tables for the dry and the wet season.

Figure 3.2 presents part of the simulated and observed hydrograph at Dwaalhoek for the selected wflow-sbm model. More monthly and annual model output can be found in Supplementary Material A. The model simulates higher total annual and monthly runoffs than observed. This is mainly caused by an overestimation of the high peak flows, and a slight overestimation of the baseflows. Calibration to low flows by increasing the saturated hydraulic conductivity leads mainly to the elimination of small peak responses, quick recession times, and even higher peak flows. This in its turn brings forward the start and end of the dry season by approximately one month, resulting in the fact that the model considers September as the driest month instead of October. Model performance differs per location: the difference between observed and modelled flows is smaller in the mainstem- and downstream, than at locations with small upstream areas such as Zandrivier and Blakeney. As can be seen in Table 3.1, the lowest errors mainly occur at Doornspruit, especially during dry conditions.

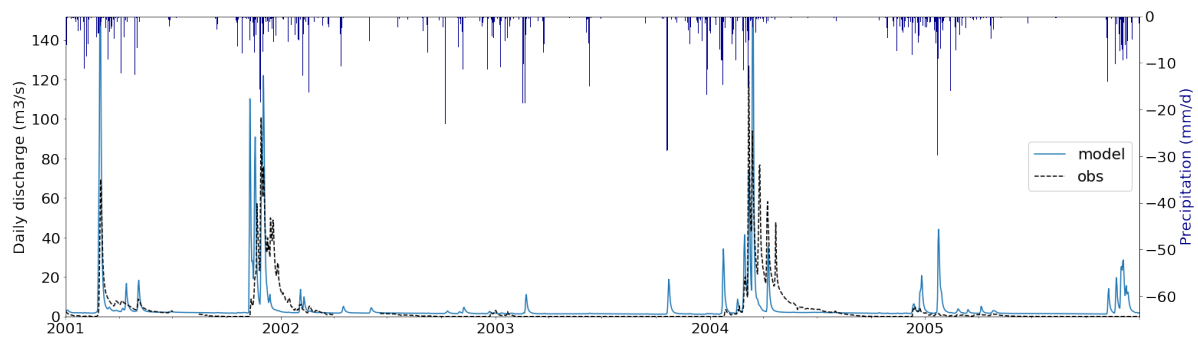


Figure 3.2 – Daily ERA5 rainfall (mm/d) and modelled and observed daily discharge (m^3/s) at Dwaalhoek between 2001 and 2006.

Table 3.1 – Model performance compared to observed flows at the four gauge stations regarding eleven metrics. Except for the Nash Sutcliffe Efficiencies (first two columns), the metrics are computed as root-mean-square errors. Daily mean refers to mean error of all daily flows between 1981-2020.

	NS (-)	NSlog (-)	Daily mean (m^3/s)	Annual mean (m^3/s)	BFI (-)	Low pulse count (-)	High pulse count (-)	Low pulse duration (d)	July mean (m^3/s)	September mean (m^3/s)	October mean (m^3/s)
Doornspruit	5.1	-10.8	0.2	0.7	0.6	72.8	44.9	17.8	0.4	0.3	0.6
Dwaalhoek	28.4	-1.8	0.1	5.2	0.6	68.4	50.9	126.4	1.7	1.4	3.5
Zandrivier	18.9	-101.7	-0.2	4.6	0.9	87.3	55.4	65.0	0.8	0.6	1.7
Blakeney	2.1	-0.7	0.0	0.5	0.8	170.1	92.0	160.3	0.1	0.1	0.2

Table 3.2 – Overview of the data used: ECMWF Reanalysis v5 (ERA5), observed precipitation from the National Oceanic and Atmospheric Administration (NOAA), streamflow timeseries from the Global Runoff Data Centre (GRDC), and climate projections from WCRP Coupled Model Intercomparison Project Phase 5 (CMIP5).

Dataset	Climate variable	Data type	Spatial resolution	Temporal resolution	Reference
ERA5	Precipitation, temperature, evaporation	Reanalysis	0.25° (30 km)	Daily (1979-2020)	Hersbach et al. (2020)
NOAA	Precipitation	Observations	5 rain gauges	Daily (1950-1997)	NOAA (2020)
GRDC	Streamflow	Observations	4 stations	Daily (1981 - 2020)	GRDC (2020)
CMIP5	Precipitation, temperature	Reanalysis	1.0-3.0° (100-300 km)	Monthly (1960-2005 and 2020-2060)	WCRP (n.d.)

3.2. Data

For this study, daily historical and projected climate and streamflow data were obtained from meteorological stations, satellites, and reanalysis studies. An overview of these datasets can be found in Table 3.2.

3.2.a. Historical climate data

The ERA5 reanalysis dataset from ECMWF provides daily precipitation, temperature and evaporation between 1979 and 2020 at a spatial resolution of 0.25° (Hersbach et al., 2020). ERA5 precipitation was compared to observed rainfall from five rain gauges between 1950 and 1997, provided by NOAA (2020). The gauge locations are shown in Figure 3.1. Monthly precipitation and temperature of the two datasets is presented in Figure 3.5. ERA5 monthly rainfall is higher in the driest months (April to October) and lower in the wet months at all five locations. The monthly relative difference with the observations varies per location and month, but was on average maximum 20%, except in June. The higher resolution dataset from CHIRPS (Funk et al., 2015) was also compared to the observed rainfall, but relative differences to the observations were found to be larger in the dry season.

As the intra-annual variability of monthly ERA5 precipitation is smaller than observed, data bias correction was applied to preserve the wide range of climate change in the stress tests. This also slightly compensates for the overestimation of dry season flow by the wflow-sbm model. Bias correction was done with monthly Empirical Quantile Mapping as described by Amengual et al. (2012). The correction was applied to the average of the observation stations, thus spatial variability was not considered. The corrected distribution can be found in Supplementary Material B.

3.2.b. Historical streamflow data

For hydrological model calibration, daily runoff timeseries from four GRDC (2020) gauge stations were retrieved. Two of them are located in the main channel (see Figure 3.1). All stations provide data for the period between 1981 and 2020. It should be noted that in some years many no flow observations are reported, especially at Blakeney. Excluding these years from the calibration did not affect the selection of the model configuration.

3.2.c. Climate model projections

An ensemble of climate projections from the World Climate Research Programme (WCRP) CMIP5 (Coupled Model Intercomparison Project Phase 5) dataset (WCRP, n.d.) was retrieved. Monthly mean precipitation and surface temperature projections between 2020 and 2080 and historical reanalysis between 1960 and 2005 were used from 26, 41, 21, and 37 models for the scenarios RCP2.6, RCP4.5, RCP6.0, and RCP8.5 respectively. An overview of the GCMs included in this study can be found in Supplementary Material C.

3.3. Historical climate trends & future projections

Historical and future climate data were consulted about a plausible range of climate change in the Mokolo region. This information forms the basis for the range of climate projections in the setup of the climate stress test (see Figure 3.4). Also, it helps to understand the hydrological behaviour of the Mokolo better and supports the selection of environmental flow indicators.

For the climate analysis, historical climate data and GCM projections were used. A Mann-Kendall trend test for monotonic trends (Mann, 1945; Kendall, 1975) was performed on spatial averages of ERA5 data, rainfall and discharge observations, and historical GCM simulations. Statistically significant climate trends occur for a p-value lower than 0.05, according to the Mann-Kendall trend test. In addition, CMIP5 projections were used to give a first indication of the plausible range of future climate change. Figure 3.3 shows the relative change in annual precipitation and temperature for the individual CMIP5 models under different scenarios. It shows a big range of uncertainty for climate projections in the Mokolo. Though, in general, the more extreme scenarios project a warmer and drier climate.

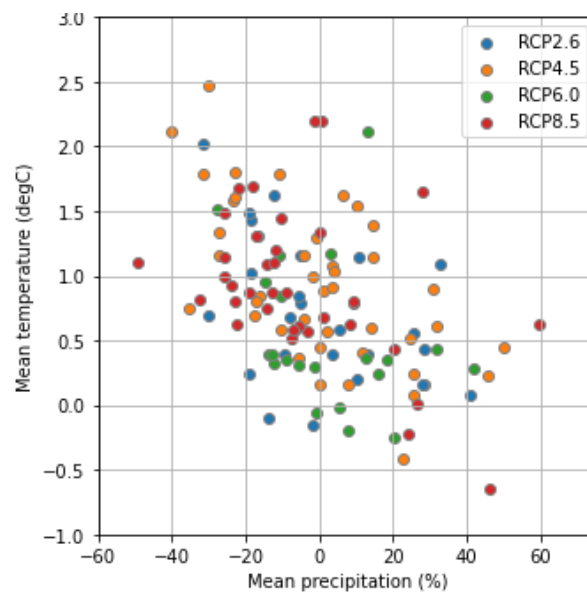


Figure 3.3 – Relative average annual temperature and precipitation changes between 1960-2000 and 2020-2060 for all individual GCMs. The density of the model projections is shown on the sides (top: precipitation, right: temperature).

3.4. Environmental flows

This study tested how the concept of environmental flows (eflows) contributes to the assessment of the Mokolo's performance under climate change. The application is moreover evaluated to whether decision scaling is a suitable framework for the concept of eflows. The workflow consisted of three steps that are presented in Figure 3.4. First, it was investigated what generic eflow indicators are available for rivers under climate change. Then, indicators that can be applied as performance indicators for decision scaling in the Mokolo were selected from this list. Finally, the selected indicators were evaluated with three requirements of the eflows concept.

3.4.a. Existing environmental flow indicators

Three types of sources were consulted to get an overview of existing eflow indicators and corresponding thresholds: scientific literature, technical reports or guidelines from local governmental or research institutions, and local stakeholders. The latter two help to determine indicators and thresholds that are specific for the Mokolo.

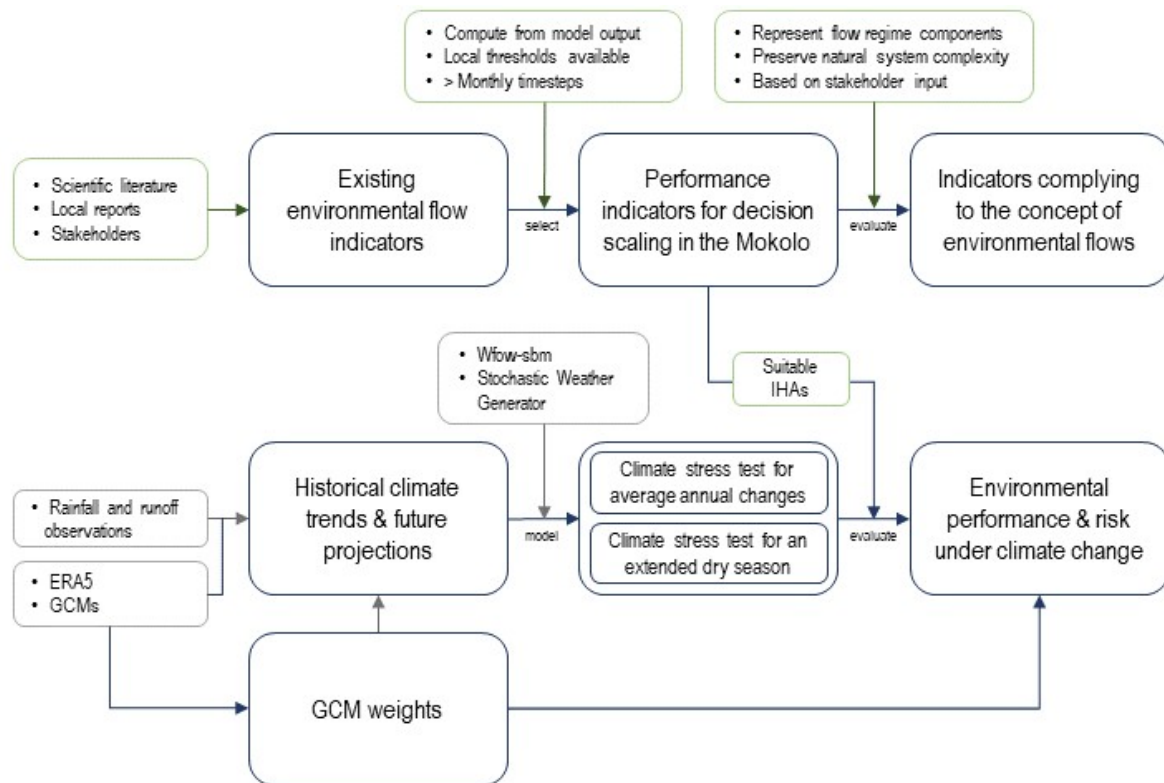


Figure 3.4 – Workflow diagram for decision scaling, including environmental flows, GCM weighting, and an additional stress test.

Scientific literature

The 32 Indicators of Hydrologic Alteration (IHA) of Richter et al. (1996) are commonly used by hydrologists and freshwater ecologists to assess the alteration of different streamflow components for ecosystems over time (e.g. in Penas et al. (2016); Li et al. (2020)). They could thus be considered as environmental flow indicators and are therefore adopted as indicators for this study. The IHA's are presented and explained in Table 3.3. Although more hydrologic indices to characterize ecologically relevant river flow regime components exist, Olden & Poff (2003) highlighted redundancy among the indicators due to multicollinearity. They did this by identifying and reviewing 170 hydrological indicators that have been used in literature. Hence, the 32 IHAs in this study are considered to sufficiently represent the different streamflow components.

Technical reports and guidelines

Streamflow requirements for the Mokolo River were found in the River Quality Report of Department of Water and Sanitation (2017). Monthly maintenance flows (30th percentile) and drought flows (5th percentile) for different locations within the Mokolo River were given. These were determined based on the South African National Water Act (1998) where every river has been assigned an annual and monthly minimum flow requirement for water quality that meets the basic human needs in a reserve and the protection of water ecosystems. In this study, drought flows were not considered, as they are not well represented by the hydrological model (see Section 3.1). As Dwaalhoek is located centrally in the main stem, and because flow simulation is relatively good there, maintenance flow requirements for that region were used as environmental flow indicators.

Table 3.3 – Overview of the Indicators of Hydrologic Alteration (IHA) from Richter et al. (1996), divided into five parameter groups linked to the flow regime components. Low pulse and high pulse refer to the flows below the long term 25th and above the 75th percentiles respectively. The table is adopted from Li et al. (2020). The bold indicators are used as performance indicators in the climate stress test.

IHA Parameter Group	Hydrologic Parameters
1. Magnitude of monthly water conditions	Mean value for each calendar month: mean flow in January; mean flow in February; mean flow in March; mean flow in April; mean flow in May; mean flow in June; mean flow in July ; mean flow in August; mean flow in September ; mean flow in October ; mean flow in November; mean flow in December
2. Magnitude and duration of annual extreme water conditions	1-day minimum; 3-day minimum; 7-day minimum; 30-day minimum; 90-day minimum; 1-day maximum; 3-day maximum; 7-day maximum; 30-day maximum; 90-day maximum; Base Flow Index (7-day minimum flow/mean flow for that year)
3. Timing of annual extreme water conditions	Day of year of each annual 1-day maximum: date of minimum; Day of year of each annual 1-day minimum: date of maximum;
4. Frequency and duration of high and low pulses	Number of low pulses within each water year: low pulse count ; Mean or median duration of low pulses (days): low pulse duration ; Number of high pulses within each water year: high pulse count ; Mean or median duration of high pulses (days): high pulse duration
5. Rate and frequency of water condition changes	Mean of all positive differences between consecutive daily values: rise rates; Mean of all negative differences between consecutive daily values: fall rates; Number of hydrologic reversals: numbers of reversals

Local stakeholders

A stakeholder meeting was held after performing the climate analysis as described in Section 3.3, setting up the hydrological model, and executing an example stress test. The preliminary results could be presented to the stakeholders to show how decision scaling works, discuss the first findings, and give context to the environmental flow indicators. Furthermore, a brief general introduction on environmental flows and performance indicators was given. After the presentations, a discussion was held by asking three questions that were synthesized from the decision scaling steps and the environmental flows concept:

- “Do you recognize the preliminary results in terms of historical climate, climate trends, river flow behaviour, and the basin’s sensitivity to climate change?”
- “What are your concerns for the Waterberg Biosphere Reserve regarding the environment and water availability? What role do climate change and human activities play?”
- “What type of river flow requirements (e.g. minimum/maximum flow throughout the year, or during the dry season, minimum/maximum duration of the dry/wet season) do you consider important for the Mokolo?”

Due to COVID-19 measurements, the meeting was organized online. Originally, it was aimed to have a broad audience present in terms of policymakers, water users, and scientists such as hydrologists, (freshwater) ecologists, morphologists and climate experts to have a good understanding of the different climatic and ecological concerns. Eventually, nine local stakeholders were present, amongst whom were two hydrologists, one agroecologist, and two zoologists. The other four were program coordinators: two from the Waterberg Biosphere Reserve, one from SANParks National Parks, and one from South African biospheres. Only the hydrologists and one zoologist were researchers by profession. Two observers were present to confirm the documentation of the meeting afterwards.

3.4.b. Selection of performance indicators

The selection of eflow indicators that are useful as performance indicators in the stress tests was based on three preconditions given by the decision scaling approach: (1) it should be possible to calculate the eflow indicators with the available model (wflow-sbm) output, (2) corresponding local performance thresholds need to be available to quantify climate risk, and (3) the indicators should be in timesteps of at least one month. The latter condition follows from the fact that GCMs can only provide plausibility of risk for monthly changes in climate conditions. Therefore, climate stress tests should be performed at similar timesteps. Evaluating flow performance indicators at smaller steps would then be irrelevant.

3.4.c. Compliance to the concept of environmental flows

The eflows concept has played an important role in the introduction of ecological components within water management projects. However, challenges in the implementation and requirements for successful application in adaptation projects have been reported (e.g. in Arnell & Gosling (2013); Arthington et al. (2006); Bunn & Arthington (2002); Poff (2018); Poff & Matthews (2013); Poff et al. (2003); Pahl-Wostl et al. (2013); Poff & Zimmerman (2010)). By addressing three frequently reported requirements for success, this research evaluated how the selected performance indicators suit the concept of environmental flows.

- Flow indicators should represent all five components of the flow regime: magnitude, timing, frequency, duration and rate of change of flow conditions (Poff & Matthews, 2013).
- When using environmental flow indicators, the natural system complexity of rivers and ecology should not be ignored in favour of finding simplistic, static, environmental flow "rules" (Arthington et al., 2006). This spatial and temporal complexity is important for ecologists. Ecological responses to flow namely vary within one river due to differences in climate and topography that facilitate different types of species (Bunn & Arthington, 2002). However, this complexity also disables ecologists to predict and quantify biotic responses of individual rivers to altered flow regimes. This in its turn challenges decision makers to translate general hydrologic-ecological principles and knowledge into specific management rules for a particular river (Arthington et al., 2006).
- Selecting environmental flow indicators should be done with the input from a wide range of stakeholders. Dialogue about sustainable water usage between a wide range of stakeholders is therefore required to map the different priorities amongst competing demands from scientists, policy-makers, water managers and users, and local populations (Pahl-Wostl et al., 2013).

3.5. Global Climate Model Weighting

The weighting strategy accounting for regional performance and independence was adopted from the approach developed and described by Knutti et al. (2017). In this strategy, each model is weighted based on how closely it resembles observed climate (performance weight) and on its similarity to other models over the historical period (independence weight). The weighting is based only on historical behaviour to avoid penalizing for convergence in the future (Merrifield et al., 2020).

The formula to compute weight w_i for model i from an ensemble of M models is as follows (Knutti et al., 2017):

$$w_i = \frac{e^{-\frac{D_i^2}{\sigma_D^2}}}{1 + \sum_{j \neq i}^M e^{-\frac{S_{ij}^2}{\sigma_S^2}}} \quad (3.1)$$

with D_i the distance metric of model i to the observations, and S_{ij} is the distance metric between model i and model j . Scaled ERA5 data at native resolution was used for the observations and the CMIP5 GCM

output was used as model data (both described in Section 3.2). The period between 1980 and 2005 and the regional extent as shown in Figure 3.1 were considered. Root-mean-square error (RMSE) was used for both distance metrics D_i and S_{ij} , which can be computed for any variable of the GCMs if observations are available. However, the selection of diagnostics should be relevant for the target, and add additional information to the other variables (Lorenz et al., 2018; Brunner et al., 2019). Therefore, three diagnostics based on monthly precipitation and temperature were selected to calculate D_i and S_{ij} : average annual precipitation (pr_{ANN}), average dry season precipitation (pr_{JJA}) and the average annual temperature (tas_{ANN}). This selection was motivated by the fact that pr_{ANN} and tas_{ANN} are input variables for the hydrological model and the stress tests, while pr_{JJA} is a relevant variable for Waterberg's drought problems. After computing the weights for each diagnostic, they were averaged in order to retrieve one weight per model.

Constants σ_D and σ_S in equation 3.1 determine how strongly the model performance and similarity are weighted. For example, a large σ_D leads closer to model democracy, and σ_S determines a typical distance when two models are considered similar. This means that if σ_S is large, models are considered dependent on each other under larger distances. If models i and j are identical, then $S_{ij} = 0$, and both models get half of the weight. It should be noted, however, that a large σ_S treats all models dependent and thus also leads to more equal weighting (Brunner et al., 2020).

For simplicity, this study used the same parameters for all diagnostics. They were determined by testing multiple combinations of σ_D and σ_S between 0 and 1. Based on previous case studies and expert judgement, the resulting $\sigma_D=0.6$ and $\sigma_S=0.3$. Most previous cases (mainly focussing on Europe and North America) of this methodology found a σ_D around 0.5 (ESMValTool, 2022). Regarding model interdependency, it is argued that shared codes lead to similar dependency on different scales (Brunner et al., 2019). Therefore, the σ_S value in this study was based on values retrieved in global assessments from Merrifield et al. (2020) and Brunner et al. (2020). The sensitivity of the parameters can be found in Figures F.2 and F.3 in Supplementary Material F, which show that σ_S has a small effect on the weights.

3.6. Climate Stress Testing

This study investigated what extra information could be provided by stress testing for changes in inter-annual variability. Therefore, two stress tests were performed. One represents average annual climate changes, a scenario that is usually examined in decision scaling. The other represents interannual changes that are environmentally relevant. As can be seen in the workflow diagram from Figure 3.4, the stress testing methodology in this study consists of three steps. First, historical and future climate data were consulted about a plausible range of climate change in the Mokolo region (detailed in Section 3.3). Based on the outcomes, the ranges of climate change for the two stress tests were determined. Subsequently, future climate timeseries within this range were simulated with the stochastic weather generator in order to maintain local weather characteristics (see the following section). The timeseries are set up by imposing climate change projections on the historical ERA5 climate data. Then, these simulations in its turn serve as forcing for the wflow-sbm model. Finally, flow performance indicators were computed with the model output to evaluate the environmental performance of the Mokolo under climate change.

3.6.a. Stochastic Weather Generator

An adapted version of the stochastic weather generator as developed by Steinschneider & Brown (2013) was used (Deltares, 2022). It can detect, based on historical timeseries of precipitation and temperature, characteristic statistics such as low-frequency climate oscillations, dry- and wet spells, and the spatial distribution of the covariance between climate variables. Parameters to linearly change the climate in the weather generator consist of monthly relative changes in temperature, precipitation and rainfall variability. The simulated output includes potential evaporation which was calculated with the Hargreaves equation (Hargreaves & Samani, 1985).

3.6.b. Climate stress test for average annual mean changes

In the first test, rainfall and temperature averages were changed equally in all months, keeping the variability unaltered. The range of change was determined based on Figure 3.3. To preserve the uncertainty range, the stress test goes beyond the range of change projected by the GCMs. The temperature was altered by six discrete increments from -1°C to 4°C , and precipitation by 15 discrete factors from -70% to $+70\%$ (see Figure 3.5). The combination of all changes gives 90 climate projections between 2020 to 2060.

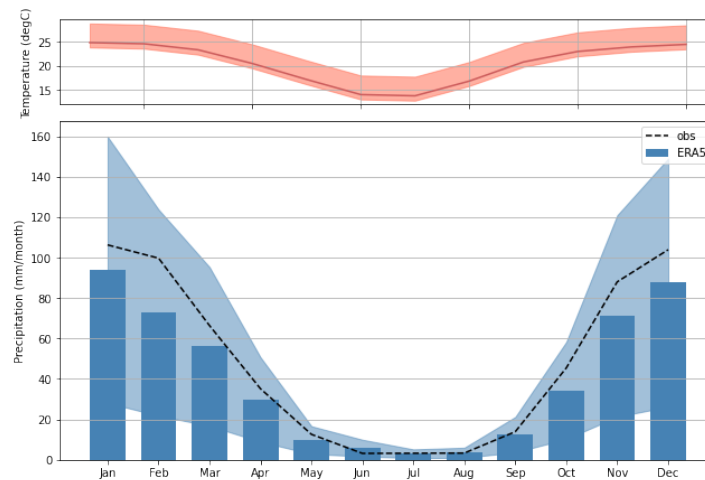


Figure 3.5 – Figures of the average historical monthly temperature (solid red line) and precipitation (bars) in the Mokolo River basin (ERA5). The range of climates that was stress tested is depicted around the historical means (temperature: -1 to $+4^{\circ}\text{C}$; precipitation: -70% to $+70\%$). The dashed line represents the average observed precipitation of the five gauge stations in the biosphere area of the Mokolo basin.

3.6.c. Climate stress test for an prolonged dry season

The second test was aimed at representing the interannual variability of climate change. However, as GCM-informed plausibility can only be assigned based on monthly values and as applying different changes per month would make it difficult to track where the river changes originate from, a relatively simple case was required. Therefore, one plausible projection according to the concentration of GCM projections in Figure 3.3 was selected as a base case: $+1^{\circ}\text{C}$ in temperature and -10% in rainfall. As dry season length is an important climate statistic for river ecology, and because trend analysis and future projections (which will further be described in Section 4.1) showed decreased precipitation at the end of the dry season, the Mokolo was tested for an prolonged dry season. Therefore, the base case was tested to a reduction of future average mean precipitation in October by -10% to -100% , with steps of 10% .

3.6.d. Performance thresholds and risk

To evaluate the impact of climate change on the performance of the Mokolo, flow performance indicators were computed with the wflow-sbm model output from the stress tests. Environmental flow indicators served as performance indicators as explained in Section 3.4.b. However, performance threshold are only reported by Department of Water and Sanitation (2017) in the River Quality Report regarding monthly maintenance flows (70% quantile). As the stochastic weather generator does not change the intra-annual rainfall distribution, the quantiles that are determined in the monthly maintenance flows do not change in the stress test. Therefore, in the impact assessment the historical monthly 70% quantile was used to evaluate how many days this threshold was reached each month. To give a broader view of the changes in the flow regime, IHAs for different components of the monthly flow regime were also computed: average annual flow, average flow in the driest months concerning rainfall and discharge (July, September, October), low pulse count, high pulse count, low pulse duration, and the Base Flow

Index (BFI). These are indicated in bold in Table 3.3. Again, the climate stress test does not influence the high pulse count and the low pulse count and duration due to the static distribution of the historical climate. Therefore, these indicators were replaced by the flows corresponding to low and high pulse thresholds (75th and 25th percentile respectively).

This chapter describes the results that were found when applying the novel decision scaling approach to the Waterberg region. First, the results from the historical and future climate analysis are presented, followed by the environmental flow indicators. Then, the weights based on GCM performance and interdependency are given and the sensitivity of the region is shown with the two climate stress tests.

4.1. Historical climate trends & future projections

An overview of statistically significant trends in historical climate data is presented in Table 4.1. Figure 4.1 shows both historical and future annual precipitation and temperature anomalies. Regarding daily and monthly temperature, increasing trends were detected in ERA5, especially at the end of the dry season (foremost in October). Likewise, Figure 4.1 shows that the multi-model mean of GCMs has been increasing over time. 16 out of the 48 GCMs showed a significant increase in annual average temperature, and no decreasing trends were found. Regarding monthly values, the highest number of increasing trends were found in October. Up to 2080, increasing temperatures are projected to continue and become more extreme according to more extreme scenarios.

Table 4.1 – Overview of historical trends in daily, monthly average, and annual average precipitation and temperature timeseries of different datasets (ERA5, GCMs, and observations). An x indicates "no trend", N/A "not applicable", and the months between brackets indicate the months when the trend occurs.

	Precipitation			Temperature	
	ERA5	Observations	GCMs	ERA5	GCMs
Daily	Decrease	Decrease	N/A	Increase	N/A
Monthly average	Decrease (Aug-Sept) & Increase (Dec)	x	N/A	Increase (Aug-Nov)	N/A
Annual average	x	x	x	x	Increase

Significantly decreasing daily rainfall and annual rain days (from 271 to 253 d/yr) were found in the observations and ERA5 dataset. Decreasing trends in ERA5 were again mainly found at the end of the dry season. An increasing rainfall trend was found in December. Average annual trends were not detected, which is in line with the historical reanalysis from GCMs in Figure 4.1. This figure moreover shows that precipitation projections are more spread than temperature, but the multi-model median for the RCP8.5 scenario slightly decreases. Although rainfall has been decreasing, daily discharge observations have been increasing at all gauges except at Zandrivier. Increasing trends were also found in the monthly runoff during the dry season (April-October) at Doornspruit and Blakeney.

Monthly GCM projections are included in Supplementary Material D. Differences between monthly temperature projections are small, and all monthly temperatures are projected to increase by up to 3° C under all scenarios, based on the interquartile ranges. Monthly multi-model medians of rainfall projections decrease for each scenario and month (except in January and December for RCP6.0). In line with historical data, seasonal projections show a larger change in the dry season than in the wet season (illustrated in Supplementary Material D). Also, the correlation between RCP scenarios and changes is clearer in the dry season.

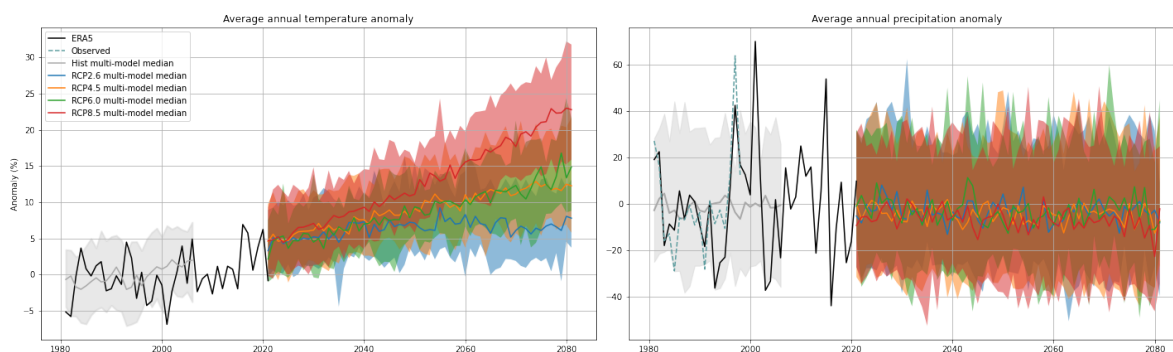


Figure 4.1 – Precipitation and temperature anomalies relative to 1980-2005 for the ERA5 dataset, the multi-model median of the GCMs, and the observed precipitation, together with the 90% ranges for all historical and future GCMs.

4.2. Environmental Flows

Table 4.2 presents an overview of the existing eflow indicators from scientific literature (IHA's) and local reports used in this study. Stakeholders did not mention specific flow indicators, and thus this source is excluded from the table.

4.2.a. Local stakeholder discussion

The responses and remarks to the questions asked during the stakeholder discussion (as listed in Section 3.4) can be summarized as follows.

- The participants recognized the detected historical trends in climate change (see Section 4.1). They illustrated this by mentioning that they observed parasites in animals and plants dying off because of hotter summers. Also, they are experiencing longer droughts that lead to dips in the boreholes used for drinking water. Changes in river flows were not explicitly mentioned.
- The participants drew attention to the fact that the Waterberg is a region with very sporadic and location-dependent rainfall events due to the steep terrains, which are too local to be represented in models.
- Their concerns about water availability were illustrated by the competing demands in the region. Currently, they are already facing dips in their groundwater wells, and platinum mining puts more pressure on that. The mining activities namely consume much water and go together with an increasing amount of labour immigrants and new infrastructure for transportation which leads to higher water demands and changes in land use. On top of that, more and more tourism lodges are being constructed in the region which will also increase the water demand.
- The participants were not familiar with environmental flows that represent flow dynamics. They rather associated the concept with water quality, which is in line with local studies and reports on freshwater ecology. Those merely focus on water quality rather than water quantity (e.g. de Klerk et al. (2016); Maeko (2020)). The stakeholders recalled that minimum requirements should be available based on the National Water Act. One hydrologist guessed that this lies around 20% of the annual mean flow for the Mokolo, based on his previous experience with other rivers in the Limpopo Province. As they are just setting up monitoring studies in the Waterberg Biosphere Reserve, they were not able to report eco-hydrological relations or indicators which was also reported in other case studies (e.g. in Poff & Zimmerman (2010); Bunn & Arthington (2002); Arthington et al. (2006)).

4.2.b. Selection of performance indicators

The overview of eflow indicators in Table 4.2 also shows which indicators comply with the preconditions of performance thresholds in this study. It becomes clear that scientific literature provides more diverse indicators in terms of statistics and time steps than the local sources. Still, all 32 IHAs from Richter et al. (1996) and the maintenance and drought flows from Department of Water and Sanitation (2017) can be computed with wflow-sbm model output. However, local thresholds are only available for monthly maintenance and drought flows. Therefore, the IHA's cannot be used as local performance indicators in the Mokolo. Maintenance and drought flows are at monthly timesteps and thus suit all boundary preconditions to be applied as performance indicators. Regarding IHAs, the mean monthly flows and 90-day minimum and maximum flows are indicators with timesteps of at least one month.

Table 4.2 – Overview of environmental flow indicators found in literature and local reports, evaluated against the three boundary conditions given by this study approach.

Source	Indicators	Compute with wflow	Thresholds available	Monthly
Literature (IHA's)	Mean monthly flows; 1-, 3-, 7-, 30-, 90-day minimum/maximum; base flow index; date of minimum/maximum; low/high pulse count; low/high pulse duration; rise rates; fall rates; number of reversals	all	-	Mean monthly flows; 90-day minimum/maximum
Local reports	Monthly maintenance flows & drought flows	all	all	all

4.2.c. Compliance to the concept of environmental flows

The three requirements from the concept of eflows as described in Section 3.4 are not met by the selected performance indicators (maintenance and drought flows). In the first place, only one component of the flow regime (magnitude of flow) is represented by the indicators. Moreover, the set of indicators only covers monthly flows at in one part of the river, so does not consider the spatial dimensions of the Mokolo. The natural system complexity is thus not preserved. Lastly, no indicators resulted from the stakeholder meeting, and the selection of maintenance and drought flow indicators as performance indicators was not done in consultation with a wide range of stakeholders. The group of stakeholders did not represent policy-makers, users, or local inhabitants, but their responses detailed above do indicate that their interests and priorities lie in managing the human activities rather than freshwater ecology.

4.3. Global Climate Model Weighting

Figure 4.2 presents the performance distance metric σ_D of the GCMs regarding the three diagnostics (pr_{ANN} , pr_{JJA} , tas_{ANN}). It shows that each model performs differently compared to the observations, but also that their performance differs per diagnostic. This indicates that the selected diagnostics are uncorrelated, which is substructured by Pearson correlation coefficients of 0.29 (pr_{ANN} - pr_{JJA}), 0.39 (pr_{ANN} - tas_{ANN}) and 0.26 (pr_{JJA} - tas_{ANN}). A correlation heatmap can be found in Figure F.1 of Supplementary Material F. It was found that, compared to ERA5, all GCMs underestimate tas_{ANN} , most GCMs underestimate pr_{ANN} , and all overestimate pr_{JJA} .

Figure 4.3 shows the interdependence distance metrics σ_S of the GCMs. The figure shows that a high model correlation regarding one diagnostic does not implicate a high correlation for another. A relation between σ_S and the similar model names could be found. Comparing Figures 4.2 and 4.3 shows that models with large RMSEs regarding ERA5 also have large RMSEs regarding other models.

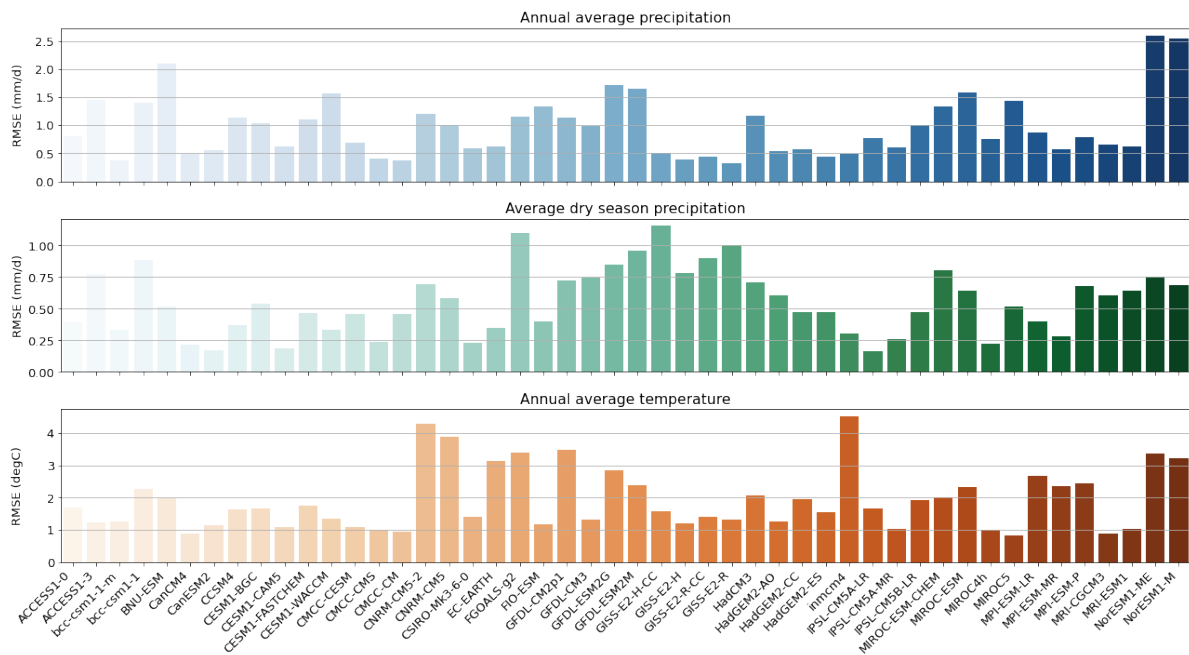


Figure 4.2 – RMSE between GCMs and ERA5 concerning annual average precipitation, dry season average precipitation, and annual average temperature.

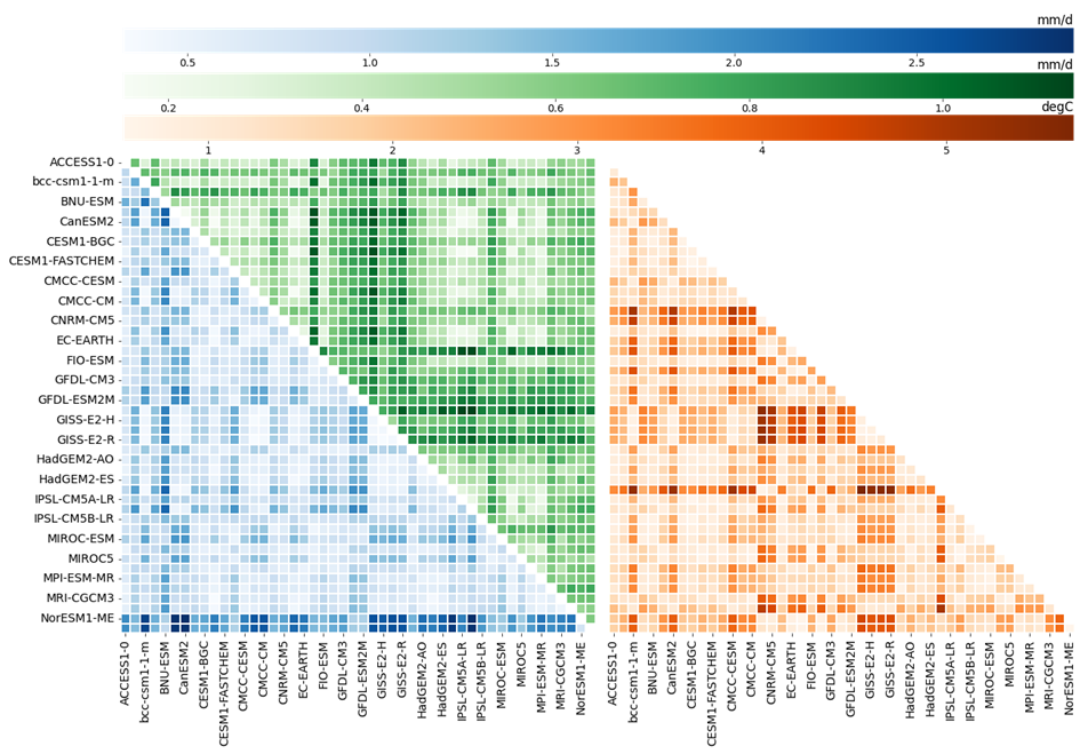


Figure 4.3 – RMSE between GCM's concerning annual average precipitation (blue), dry season average precipitation (green), and annual average temperature (orange).

The resulting relative weights per model can be found in Figure 4.4. When applying these weights to each diagnostic, it was found that the median relative changes from all GCMs decrease (see Figure 4.5). For annual and dry season precipitation, the range of model projections narrows, but widens for

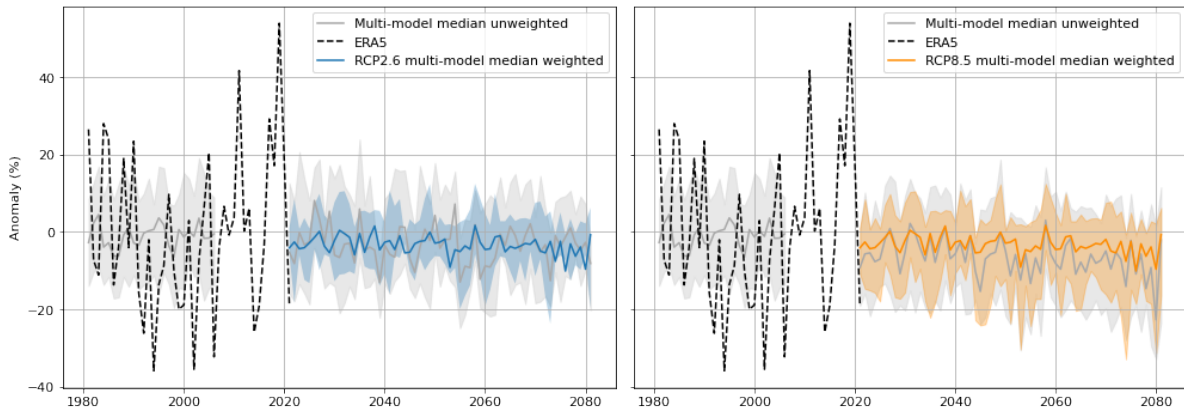


Figure 4.7 – Time series of weighted and unweighted precipitation projections for 2020-2080 relative to 1980-2005 under RCP2.6 and RCP8.5. The shaded area represent the interquartile range.

The impact of weighting for combined precipitation-temperature projections can be found in Figure 4.8. By comparing the weighted and unweighted density distributions, it can be seen that weighting leads to more similar projections between the RCP scenarios. The projections shift towards less relative change. Also, the weighted distributions of precipitation projections are similar under all scenarios, whereas the density of weighted temperature projections decreases under all scenarios, except for RCP2.6. This is in line with the changes in range of uncertainty due to weighting which were also found from Figures 4.5, 4.6 and 4.7. Also, lower weights seem to be assigned to models projecting a decrease in precipitation and a moderate increase in temperature (bottom left in the figure), and to models projecting increasing precipitation with increasing temperatures (top right in the figure).

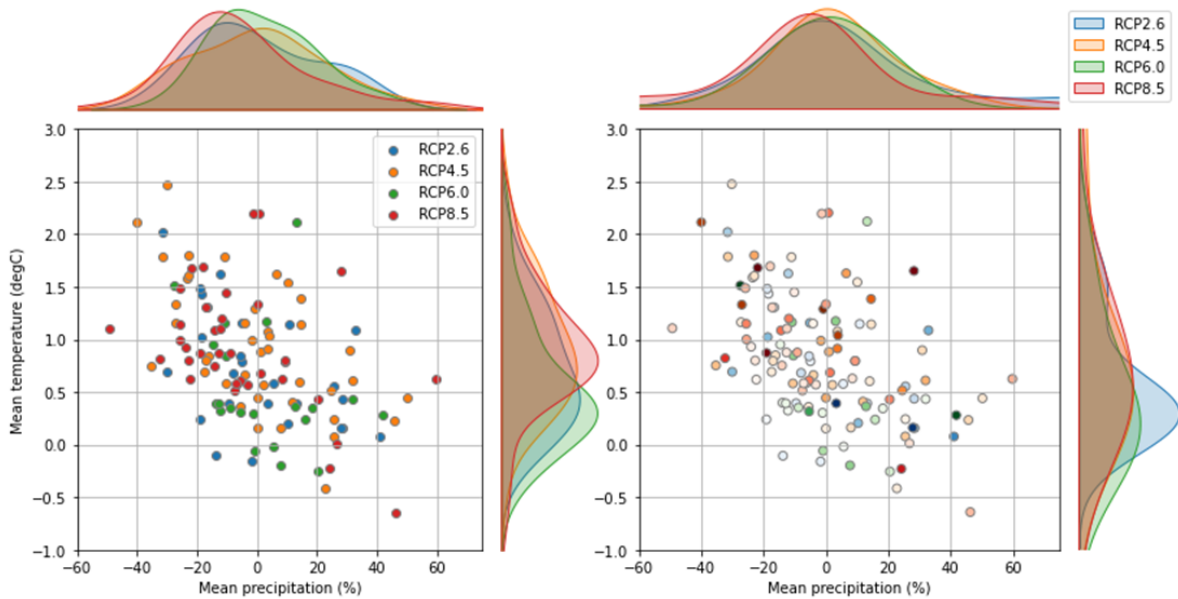


Figure 4.8 – Relative average annual temperature and precipitation changes between 1960-2000 and 2020-2060 for all individual GCMs. In the right figure, the model weights are indicated by the darkness of the colors. The weighted density of the model projections is shown on the sides (top: precipitation, right: temperature).

4.4. Climate Stress Testing

The Mokolo River basin was stress tested with two types of tests: one for testing the impact of changes in annual means and one for testing the impact of an prolonged dry season. This section shows the stress test results and subsequent changes in flow performance at Dwaalhoek (see location in Figure 3.1). The plausibility of climate conditions is shown with weighted GCM projections.

4.4.a. Climate stress test for average annual mean changes

Figure 4.9 shows the annual mean flow change at Dwaalhoek for the changes in precipitation and temperature that were imposed by the climate stress test. It can be seen that average flow is significantly more sensitive to changes in precipitation than temperature. Moreover, it responds linearly to temperature changes and seems to respond quadratically to precipitation changes. Absolute flow changes are thus larger for increasing precipitation than for decreasing precipitation. Figure 4.10 presents the historical and future annual mean flow and precipitation anomalies over time. It shows that the precipitation anomalies from the stress test lead to much higher future discharge anomalies.

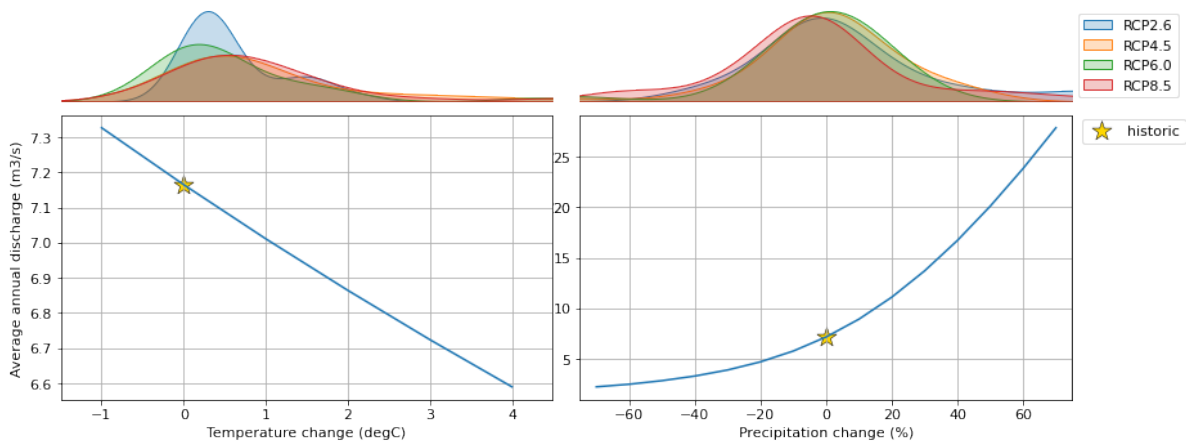


Figure 4.9 – Annual mean flow response to changes in temperature (left) and precipitation (right) between 2020-2060 relative to 1980-2020. Note that the vertical axes are different. The yellow star indicates the average historical river flow and climate conditions. The distributions of average temperature and rainfall projections between 2020-2060 from GCMs are given in the upper figures.

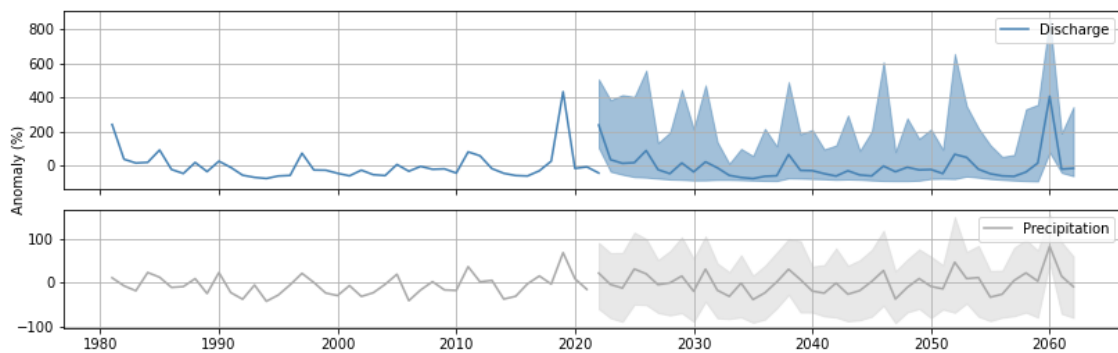


Figure 4.10 – Time series of annual mean discharge (top) and precipitation (bottom) anomalies relative to 1980-2020. The shaded area represent the 90% range.

Figure 4.11 combines precipitation change, temperature change, and the corresponding flow changes in one image. This is presented for all flow indicators. The images show that all indicators respond similarly to climate change: they are more sensitive to precipitation than temperature changes, and flow changes are larger under increasing than decreasing precipitation. The contrary applies to the

Base Flow Index, as groundwater influence becomes larger under drier climates. Additionally, some indicators are more sensitive than others. In Supplementary Material E this is illustrated by expressing the relative flow responses. It was found that the average annual flow, the flow in October, and the low- and high pulse thresholds have the largest range of relative change under these climates. The Base Flow Index showed the least relative change.

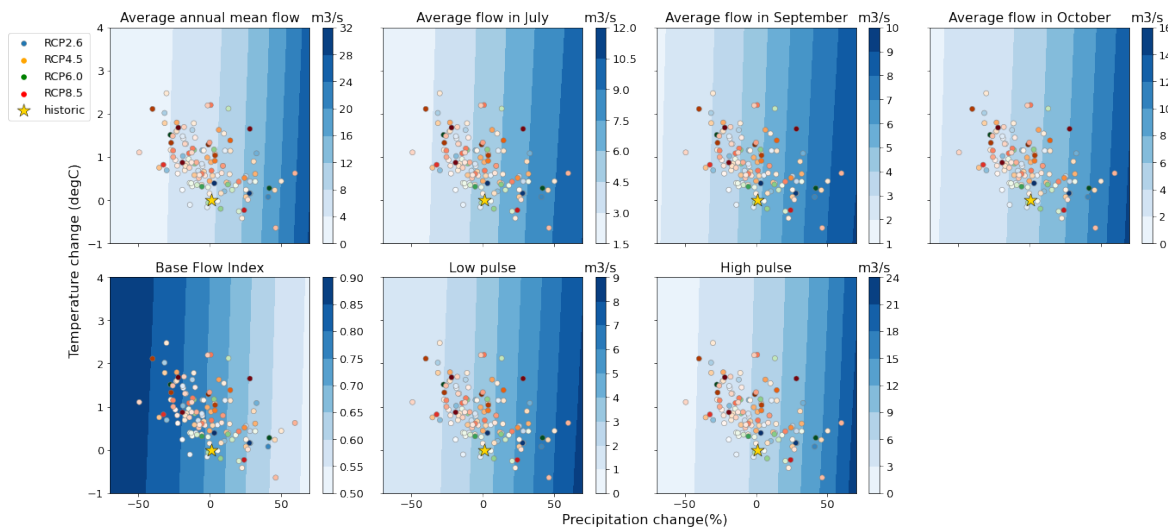


Figure 4.11 – Responses to temperature and precipitation changes for seven flow indicators at Dwaalhoek. The temperature and precipitation changes indicate relative changes between historical (1980-2020) and future (2020-2060) conditions. The yellow star indicates the historical river flow and climate conditions. Climate projections from different GCMs under different RCP scenarios are indicated with dots. Note the different bar ranges and units.

4.4.b. Climate stress test for an prolonged dry season

Figure 4.12 presents the response of eflow indicators and monthly discharge to drier October months. It should be noted that the results are based on an already drier climate (-10% annual rainfall). From the figure, it can be seen that a rainfall decrease of -90% or -100% has almost similar output regarding the eflow indicators and monthly flows. Eflow indicators show relatively more response up to -60% than for more severe changes. Moreover, low pulse response is the largest, and the Base Flow Index and high pulse response are the smallest. The monthly flow changes show that October rainfall influences flow throughout the entire year, but the magnitude of the impact relates to the order of the posterior months. January however, shows a larger response than December. When October rainfall decreases by more than 70%, January flow is more impacted than November flow. Under more than 80% decrease, February is more impacted more than December. Monthly flows in March to September are impacted similarly. Lastly, it was found that the climate impact on monthly flows increases over time between 2020 to 2060.

4.4.c. Performance thresholds and risk

Figure 4.13 presents how the monthly number of days below the historical 70% quantile changes under average annual climate change. It can be seen that again temperature changes have hardly any impact and that the sensitivity in each month is similar. Moreover, it was found that from -50% to +40% precipitation change, the entire monthly flow regime can shift from all flow below the 70% quantile to all flow above the 70% quantiles. This can be illustrated as follows. Under historical conditions, nine to ten days per month have flows under the 70% quantile. Thus, when precipitation increases by more than 40%, the number of days below the threshold drops by nine days, which means that river flows does not drop under the 70% anymore. The contrary applies for extremely decreasing scenarios (<-50%) in March, May, July, August, and December.

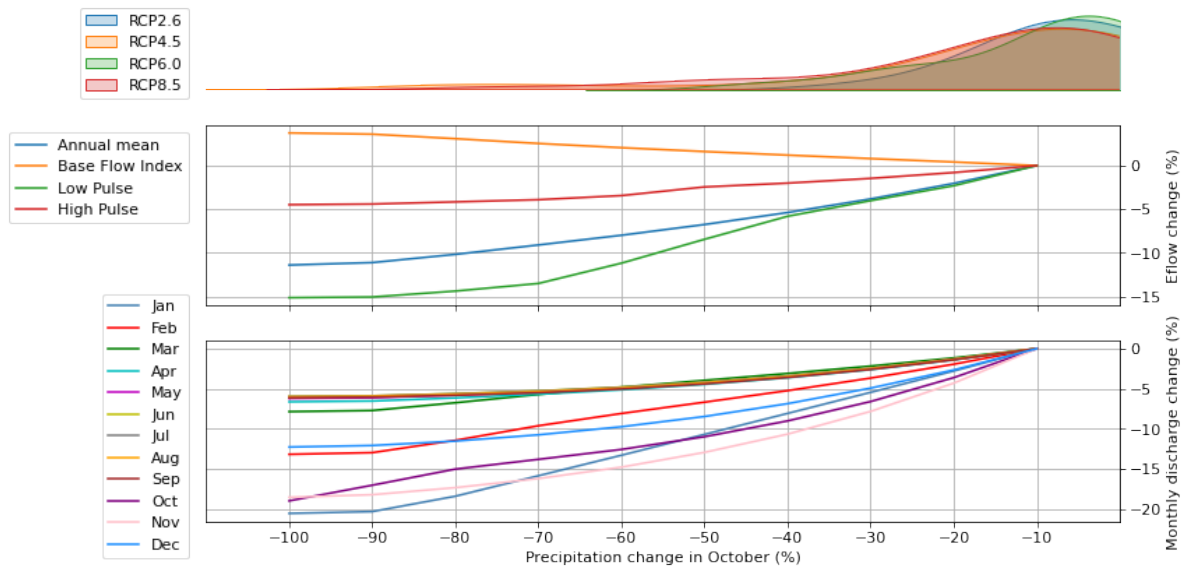


Figure 4.12 – Flow response of eflow indicators (middle) and monthly flow (bottom) to a prolonged dry season, relative to the base case: the average historical climate conditions (1980-2020) imposed with -10% rainfall. The density of GCM projections for October rainfall changes under the four RCP scenarios is shown on top.

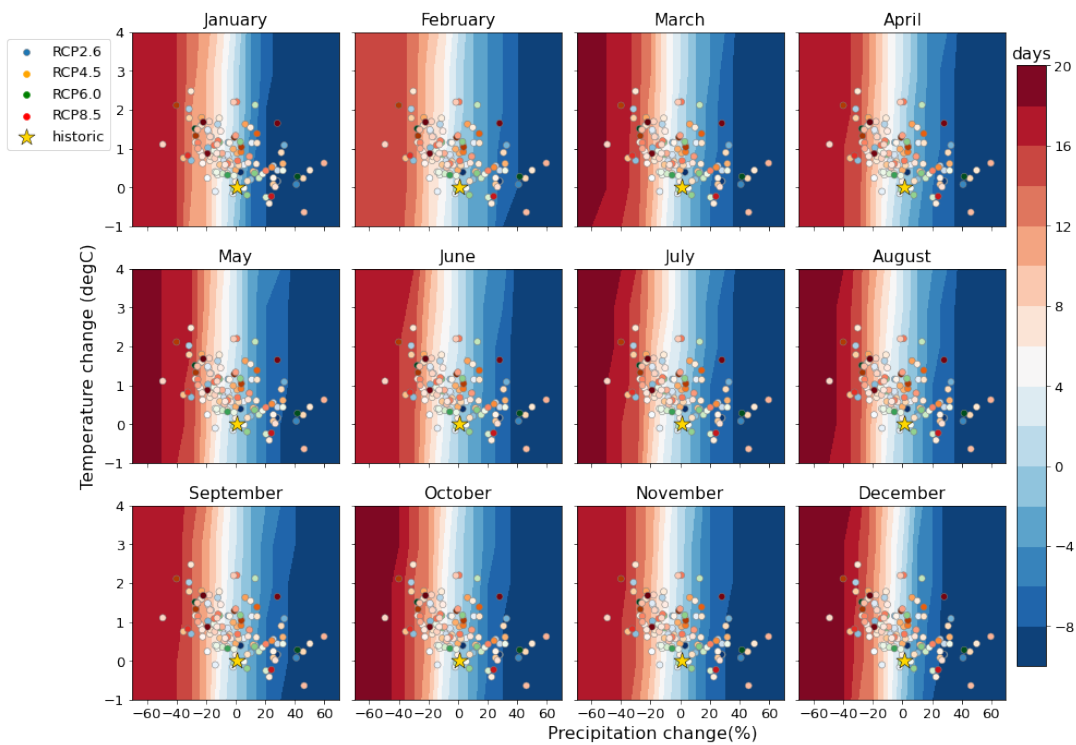


Figure 4.13 – Response of the number of days with flow under the historical monthly 70% quantile to different climate changes. The number of days is indicated relative to the historical number of days. Red colours indicate a relative increase and the blue colours indicate a relative decrease.

Application of the adapted decision scaling approach to the Waterberg region showed large uncertainties in future climate behaviour and river response. This highlights the importance of performing such a vulnerability assessment for robust decision making, as was also emphasized by Haasnoot et al. (2013); Kwakkel & Haasnoot (2019); Shortridge & Guikema (2016); Verbist et al. (2020). However, the study results also suggest that their strong model-dependency in terms of spatially distributed data, the hydrological model, stochastic weather generator, and GCMs, leads to an oversimplification of local climate variability, characteristics and needs when applying to a real case. This will be further elaborated on and discussed in the following sections.

5.1. Data

Although data uncertainties were beyond the scope of this study, it should be noted that the results are highly dependent on the ERA5 reanalysis dataset, and the precipitation and discharge observations. The climate analysis, model calibration, stochastic weather simulations, and GCM weighting are namely all based on these datasets. ERA5, however, results from a reanalysis model that uses downscaling and data assimilation techniques which might not capture local climate phenomena at resolutions less than 30 km, such as the rainfall sparsity and spatial variability that were found to be an important characteristic of the Mokolo area (see Section 4.2).

ERA5 bias correction was therefore introduced to preserve the higher interannual rainfall variability from the observations. This could moreover reduce the overestimated dry season flow from the hydrological model. However, the application of empirical quantile mapping might have led to overfitting and overconfidence in the observational dataset. It should be noted that subgrid spatial variability of observed rainfall was not considered which could have influenced the infiltration and runoff times. On the other hand, the rain gauges and the spatially averaged rainfall were observed to be well correlated with Pearson correlation coefficients for rainfall coincidence all above 0.5. On top of that, this research mainly focussed on discharge changes at monthly timesteps which are not affected by these processes on a small timescale, especially given that the hydrographs already showed short runoff response times to rainfall. When examining the impact of climate change and land use change on discharge at smaller timesteps, spatially distributed rainfall could however play a more important role.

To reduce the risk of overconfidence in observations or reanalysis models, and to preserve spatial variability, it is recommended for climate scientists and decision makers to prioritize local data collection in data scarce environments such as the Mokolo. Up to then, it could be fruitful to use multiple global datasets likewise ERA5 (e.g. NCEP, MERRA, CFSR) for model setup and simulations, and GCM weighting. The latter was also advocated by Lorenz et al. (2018) and Brunner et al. (2020). A similar GCM weighting strategy as suggested in this study might even be explored for those historical reanalysis datasets. Moreover, uncertainties in climate variability could be simulated with the stochastic properties of the weather generator which were not employed in this study. Whateley et al. (2016), for example, tested a water supply system for almost 4000 stochastic timeseries in three climate scenarios to represent the wide range of variance uncertainty for robust climate adaptation.

5.2. Hydrological model

This study found that the flow regime of the Mokolo was difficult to represent in wflow-sbm, due to the quality of the observations, small scale climate- and geographical characteristics, and human interference with the river. Therefore, the results of this study emphasize that in decision scaling the climate sensitivity of one model configuration is stress tested rather than the actual basin. The wflow-sbm model is based on a simplified unsaturated zone component (Schellekens et al., 2021) and as groundwater flows are dominating in the arid and sandy Mokolo catchment, this simplification was plausibly limiting

the model performance of the region. In addition, hydrologists widely acknowledge the challenge of river runoff simulation in arid and semi-arid catchments (e.g. (Koch et al., 2020; Mengistu et al., 2019; Liu et al., 2021; Qureshi et al., 2022)). Other modelling studies of the basin and its surroundings also reported unsatisfactory performance due to a lack of qualitative rainfall- and groundwater data and a poor understanding of the geology (e.g. in Seaman et al. (2016), Prucha et al. (2016)). Kundzewicz et al. (2018) did therefore suggest using multiple model configurations, rather than the best model concerning the historical performance, to evaluate the impact of climate change in different seasons. In climate stress tests, this should however be carefully adopted as model equifinality could divert to bad model performance under climate change.

On the other hand, various studies (e.g. (Gosling et al., 2011; Kundzewicz et al., 2018; Her et al., 2019)) have stated that it is better to focus on the uncertainty in climate model projections than in hydrological models as the latter was found to be rather small. Steinschneider et al. (2022) for example found that the contribution of their systems model error to total uncertainty is approximately 5-15% relative to climate based uncertainties. Likewise, in this study, the RMSE between modelled and observed annual average flow at Dwaalhoek is 5.2 m³/s, whereas the most extreme GCM projections lead to a difference of almost 32 m³/s (see Figure 4.11). Other flow metrics also show a difference of approximately a factor of six. This factor was found to remain the same when stress testing with the uncalibrated wflow-sbm model. However, it is important to mention that this comparison does not involve the quality of the observations and the hydrological model performance under future conditions. To validate whether a simplified systems model is sufficiently accurate to use in climate vulnerability assessments, Steinschneider et al. (2022) developed an approach based on variance decomposition in decision-relevant metrics for comparison to other sources of uncertainty, such as the choice of GCM, RCP, and the interaction between them. Such an approach however involves GCM model output at a daily time step, and thus requires temporal disaggregation techniques, which is tried to be avoided in decision scaling. Additionally, Pastén-Zapata et al. (2022) assigned weights to hydrological models based on their robustness under changing climate conditions. This helped to better understand the uncertainty of the projections and increased the reliability of the climate change impact assessment.

5.3. Environmental flows

This study demonstrates that the limited local knowledge of eflows in the Mokolo and the preconditions imposed by the model approach narrow the number of eflow indicators that are suitable as performance indicators. This suggests that the selection of indicators oversimplifies the river dynamics, which disables fulfilment of requirements for successful eflows application. This is in line with the challenges of implementation reported in previous studies (e.g. Arnell & Gosling (2013); Arthington et al. (2006); Bunn & Arthington (2002); Poff (2018); Poff & Matthews (2013); Poff et al. (2003); Pahl-Wostl et al. (2013); Poff & Zimmerman (2010)).

On the other hand, this research on eflows in decision scaling does contribute to the field of eflows with an example case study, as was called for by Pahl-Wostl et al. (2013). Besides, the findings suggest that the IHAs from Richter et al. (1996) can support decision scaling by providing indicators that give a broader view on changes in different flow regime components than the static average indicators that were usually applied in decision scaling. Although this study only adopted indicators on flow magnitude, it was still insightful to look at changes during different flow conditions, such as dry months, wet pulses, and baseflows, rather than only average annual flows. The results of the two climate stress tests showed namely that some environmental flow indicators were more sensitive than others. For example, the average annual flow and the low pulse flow threshold were most sensitive to climate change, while the Base Flow Index was most robust. The differences in sensitivity show that evaluating changes in different flow components, which can be partly captured by environmental flows, helps to understand the vulnerability of the river better.

Although the stakeholder meeting could not be used to determine indicators and thresholds, the discussion still provided valuable local information. The meeting summary indicates that there is a mismatch between the concerns of the participants, the topics that are discussed in local reports, and the models and indicators that were used in this study. The stakeholders were namely focused on the impact of land use change, groundwater extractions and drinking water availability from groundwater resources, whereas the IHAs and wflow-sbm examine ecological and surface flow changes. As explained in the

previous section, wflow-sbm model is not suitable for assessing groundwater impact, and the model parameters were assumed to be static under changing climate conditions and human activities. Likewise the stakeholders, local reports on rivers address primarily hydrological changes due to human activities (e.g. Maeko (2020); Lyon et al. (2017); Seaman et al. (2016)). The Mokolo's "State-of-Rivers Report" (River Health Programme, 2006) does cover environmental issues such as longitudinal dysconnectivity, invasive species in the riparian floodplain and habitat availability, but these are components that cannot be computed in wflow-sbm, as river dimensions and water levels are not included.

This mismatch between the local concerns, model objectives and indicators means that the questions of the stakeholders could not be answered by this study adequately. It could moreover explain the underperformance of the hydrological model, which suggests that human impact might be of more influence on water availability than climate change. It was for example observed that some rivers experienced an increasing flow trend, although rainfall was decreasing. This may be explained by dam control and land use changes leading to higher runoff coefficients. In addition, DWS (2015) reported that the total water requirement in the Mokolo catchment was 8 mm/yr in 2015, from which two-third is used for irrigational use and 7% is extracted from groundwater. For comparison, the annual river flow is 30 mm/yr, 5% of the annual rainfall. The stress test results showed that a rainfall decrease of 10% (-60 mm/yr) within 40 years is very likely to occur and decreases the annual river flow by 20% (-6 mm/yr). These numbers show that the impact of climate change, future groundwater availability and population increase are relevant concerns.

For more insight into the human impact and groundwater resources in the Mokolo, using groundwater indicators such as drought duration and groundwater deficit, and developing a water allocation model, groundwater model, or 3D-river model is recommended. Additionally, the wflow-sbm model could be enhanced with a water extraction element. Although it is a frequently used assumption that model parameters remain static under changing climate conditions and human activities (e.g. in Sperna Weiland et al. (2021); Fowler et al. (2007)), exploring the incorporation of dynamic land use changes and soil properties in these types of models would be valuable for simulating the effect of human activities (Engida et al., 2021; Lan et al., 2020). For example, multiple studies have tried to incorporate this by making use of land cover scenarios (e.g. in Dwarakish & Ganasri (2015); Gao et al. (2020); Xiong et al. (2017)), and Nijzink et al. (2016) attempted to represent deforestation with a dynamic root-zone moisture capacity. Öztürk et al., (2013) coupled their hydrological model to a land use dynamics model via the Leaf Area Index and Root Depth parameters.

It should be addressed that conclusions on the stakeholders' wishes and concerns are based on the interpretation of statements from a small group of stakeholders. In addition, as data in the region is scarce, they also had to base their statements on their perception and experiences. Other regions nearby the Mokolo that have more hydrological and environmental data available have already focused on environmental issues, substantiated by water quality and flow measurements. Future studies would therefore benefit from doing a stakeholder analysis beforehand, in order to invite a wide and knowledgeable audience to the stakeholder discussions and to have a good understanding of the available knowledge and data in the region. Moreover, as stakeholders were unfamiliar with the eflows concept, it is important to raise awareness of the relevance of eflows in river studies among local ecologists, hydrologists, and policymakers. Next, the discussion should be a basis for selecting a model that matches the concerns of the stakeholders. Collaborative, interactive or participatory modelling might be helpful to preserve the decision scaling analysis on local wishes and concerns (Basco-Carrera et al., 2017) and contributes to spreading knowledge on the eflows concept as was suggested in the previous paragraph. Such participatory methods improve the success of eflow implementation (Conallin et al., 2018) and introduce relationships with fields that are beyond biophysical sciences (Anderson et al., 2019). Videira et al. (2003), for example, applied participatory modelling to facilitate public and stakeholder involvement in environmental decision-making. They found that it improved the comprehension of the problem, the area, and enhanced institutional trust and commitment towards actions. Moreover, this type of modelling is relatively easy to introduce in decision scaling as it already involves stakeholders.

5.4. Global Climate Model Weighting

The implementation of the GCM weighting strategy from Knutti et al. (2017) led to more lower multi-model median anomalies for future precipitation and temperature, which agrees with results from previous studies accounting for model performance and correlation (Lorenz et al., 2018; Knutti et al., 2017; Brunner et al., 2020; Steinschneider et al., 2015; Kiesel et al., 2020). Moreover, it was found that the weights had a different effect on the interquartile spread of precipitation than on temperature spread. Regarding precipitation, weighting narrows the range of uncertainty similarly in all RCP scenarios, whereas the range of temperature uncertainty was increased, especially in more extreme scenarios. This suggests that the performance and correlation of GCMs are not related to the combination of rainfall and temperature they project. An increased range of temperature uncertainty was not found in other studies, but it should be noted that this is the first application to a region in the Southern Hemisphere. For example, Brunner et al. (2019) found a decreased temperature spread in Europe, likewise Lorenz et al. (2018) for summer temperature in North America, Brunner et al. (2020); Merrifield et al. (2020) for global temperatures, and Knutti et al. (2017) for Arctic temperatures. The effect on precipitation projections was only presented by Brunner et al. (2019), who also found that weighting leads to lower future precipitation anomalies. Steinschneider et al. (2015) have been the only ones so far reporting an underestimation of climate variance when not accounting for model correlations.

It should be noted that the results from this study risk overconfidence, because only one dataset and two climate variables were considered. Also, the small region size could decrease the robustness of the method (Brunner et al., 2019). These limitations are however already extensively elaborated upon in previous studies (e.g. in Lorenz et al. (2018); Knutti et al. (2017); Brunner et al. (2020); Steinschneider et al. (2015); Kiesel et al. (2020)), and will therefore not be repeated in this chapter. Moreover, to avoid penalizing for convergence in the future, the weights are based only on the historical behaviour of the models. Only the reproduction of historical means was considered which may by definition not be an indicator of future performance of simulating climate variability. Other studies have therefore suggested weighting based on the representation of historical climate trends (Sperna Weiland et al., 2021; Knutti et al., 2017; Kiesel et al., 2020). On the other hand, neglecting future GCM projections when weighting also neglects the model correlation regarding their representation of the interaction between climate variables and RCPs. This could be a fruitful extension of the strategy, as Steinschneider et al. (2022) argued that "climate uncertainty is dominated by the choice of GCM and its interactive effects with RCPs, rather than the RCP alone".

5.5. Climate stress test

In both climate stress tests, it was found that the selected indicators of the Mokolo's river flow are more vulnerable to precipitation than temperature changes. Moreover, increasing precipitation scenarios were found to influence runoff indicators more than decreasing precipitation, especially in more extreme scenarios. Although sensitivities in both tests were similar, the additional stress test contributes to the average annual climate stress test by showing the duration of climate change impact within a year. It was for example found that the impact lasts the entire year, but that the flows in November and January were the most sensitive. This means that lengthening the dry season has a relatively high impact on the total annual water availability as the posterior wet months are also impacted.

It should be noted, however, that this study was restricted by an unaltered rainfall distribution under climate change, which means that the (monthly) minimum, maximum, and mean flows changed similarly. This could explain the robustness of the Base Flow Index and the similar response of indicators and monthly flow to rainfall and temperature. Nevertheless, it also means that the results do not represent the Mokolo's climate vulnerability to inter- and intra-annual variability and rainfall extremes that are just so characteristic of climate change (see Chapter 1). It is therefore recommended to continue examining the effect of multiple climate stress tests with a focus on climate inter- and intra-annual variability and extremes. Although the plausibility and range of change in climate variability cannot be informed by GCMs, as these provide only monthly information, such tests can still give further insight into the river's climate sensitivity.

In this case study, the available knowledge and data were insufficient to determine corresponding local performance thresholds for the environmental flow indicators. The monthly number of days below the 70% quantile (maintenance flows) was in the first instance used to evaluate under what climate conditions the ecology of the Mokolo River is at risk.

These could, however, not be directly adopted to assess risk. The original maintenance flows were namely (1) based on a historical flow duration curve that does not match the output of the wflow-sbm model, (2) based on an ecosystem and a flow regime that will be altered by climate change and human activities, and thus may require another threshold, (3) setup to regulate minimum dam release in the region, which will also change under climate change and is not included in the hydrological model. In line with these findings, Acreman et al. (2014) demonstrated that the dynamic character of ecosystems asks for dynamic adaptation. This suggests that using far-future thresholds based on historical experience does actually not fit a methodology designed for robust adaptation. Moreover, the relative flow changes in the Mokolo to a wide range of changes are also useful, as Stainforth et al. (2007) already noted that information on relative changes may be just as important as detailed climate forecasts to understand the local consequences. This is especially valuable in data scarce environments such as Waterberg. It was, for example, found that average indicators such as annual flows are not necessarily less vulnerable than flows under dry conditions such as October flow. Also, groundwater contribution was relatively little influenced by climate change. This information could be valuable to determine when and where (the river or ground) to extract water.

All in all, it may thus be more important to further study the locally relevant flow indicators that provide broad information on a river's climate vulnerability and what models and data match these indicators, than to find exact indicator thresholds.

6 | Conclusion

The large uncertainty range and variable nature of climate change require dynamic adaptation strategies. Therefore, the decision scaling methodology, which links bottom-up vulnerability assessment with climate information from global models, has been developed. This study aimed to improve this methodology in the Waterberg Biosphere Reserve in South Africa by extending it with environmental flow indicators, a Global Climate Model (GCM) weighting strategy, and an additional climate stress test for interannual precipitation changes. An approach involving historical and future climate analysis, a hydrological model, a weather generator to impose climate change, and (local) expert discussions was used.

It was observed that using environmental flow indicators as performance indicators contributed to decision scaling by introducing non-static indicators that represent multiple flow regime components in addition to static averages. In this study, Indicators of Hydraulic Alteration (IHA) were adopted, together with information from local reports and stakeholders. Although the selected IHAs for the stress tests only represented average flows, and determination of corresponding thresholds to the IHAs was not possible with local data, relative changes for the different indicators did provide a broader view of the climate vulnerability of the Mokolo River. For example, a similar sensitivity in average- and low flows and a small response to climate change in the Base Flow Index were detected.

However, it should be noted that applying environmental flows in decision scaling requires clear communication with stakeholders in an early stage of the process. The stakeholder meeting namely revealed that local stakeholders are concerned about future groundwater availability due to land use changes, immigration, tourism and mining. Yet, these activities were not included in the hydrological model and IHAs. On the other hand, the combination of data scarcity and limited knowledge about freshwater ecology and local hydrology raises the question of how well the Mokolo River is protected regarding its future water availability and ecology.

This research illustrated the relevance of a weighting strategy in climate adaptation projects, as the wide uncertainty range in future eflow indicator responses asks for supportive information for decision makers. The GCM weighting strategy of Knutti et al. (2017) can be used in decision scaling to incorporate regional model performance and interdependency when evaluating the plausibility of future climate conditions. The results showed that, by applying this approach, the weighted median of GCM projections for Waterberg shifted towards less change in future precipitation and temperature. Although weighting decreased the interquartile spread of precipitation projections for all Representative Concentration Pathways (RCPs), the contrary was found for temperature projections. In this way, the weighted results showed that both an increase and decrease in precipitation are plausible to occur in the future and that future temperature remains highly uncertain. These results underline the need for preparing for both types of climate.

Stress testing for interannual changes rather than only average annual changes provides new insight into the duration and impact of the variable nature of climate change. This test was performed by prolonging the dry season by one month (October). Its impact was observed throughout the entire year, especially in the posterior wet months. Therefore, not only the low pulse quantile was sensitive to this change, but also the average annual flow. The observations show that additional stress tests in decision scaling are promising for a better understanding of the relation between local climate and hydrology and its sensitivity to climate change. Future decision scaling applications would thus benefit from performing multiple stress tests that represent the variable nature of climate change, such as inter- and intra-annual variability and changes in climate extremes by further employing the stochastic weather generator to simulate these changes.

In conclusion, the novel approach to decision scaling in the Waterberg Biosphere Reserve illustrates that application to a real case is challenging when local data is scarce, the climate and hydrology are difficult to represent in a model, and the impact of human activities on the water resources is still unknown.

Additionally, the strong dependency of the approach on models, climate data and indicators limits the representation of the local spatial and temporal variability of climate (change), ecology, hydrology and human activities. It is therefore recommended to thoroughly explore the local available knowledge, activities, and concerns before simplifying the local complexity with models and indicators. In the Waterberg region, one should prepare for future droughts that reduce the water availability, but also for wetter periods that can influence the local freshwater ecology and may offer opportunities for water storage. Moreover, water extraction regulations and monitoring could protect vulnerable communities and ecology. As local data is scarce, future climate adaptation studies and strategies in Waterberg would benefit from collecting spatially distributed runoff, groundwater, and ecological data and link this to human activities intervening with the water system.

References

- Acreman, M., Overton, I., King, J., Wood, P., Cowx, I., Dunbar, M., ... Young, W. (2014). The changing role of ecohydrological science in guiding environmental flows. *Hydrological Sciences Journal*, 59(3-4), 433-450. doi: 10.1080/02626667.2014.886019
- Amengual, A., Homar, V., Romero, R., & Alonso, C., S.and Ramis. (2012). A Statistical Adjustment of Regional Climate Model Outputs to Local Scales: Application to Platja de Palma, Spain. *Journal of Climate*, 25(3), 939-957. doi: <https://doi.org/10.1175/JCLI-D-10-05024.1>
- Anderson, E. P., Jackson, S., Tharme, R. E., Douglas, M., Flotemersch, J. E., Zwarteveen, M., ... Arthington, A. H. (2019). Understanding rivers and their social relations: A critical step to advance environmental water management. *WIREs Water*, 6(6), e1381. doi: <https://doi.org/10.1002/wat2.1381>
- Arnell, N. W., & Gosling, S. N. (2013). The impacts of climate change on river flow regimes at the global scale. *Journal of Hydrology*, 486, 351-364. doi: <https://doi.org/10.1016/j.jhydrol.2013.02.010>
- Arthington, A., Bunn, S., Poff, N., & Naiman, R. (2006, 01). The challenge of providing environmental flow rules to sustain river ecosystems. *Ecological Applications*, 16, 1311-1318. doi: 10.1890/1051-0761(2006)016[1311:tcopel]2.0.co;2
- Basco-Carrera, L., Warren, A., van Beek, E., Jonoski, A., & Giardinoa, A. (2017). Collaborative modelling or participatory modelling? a framework for water resources management. *Environmental Modelling & Software*, 91, 95-110. doi: <https://doi.org/10.1016/j.envsoft.2017.01.014>
- Brown, C., Ghile, Y., Laverty, M., & Li, K. (2012). Decision scaling: Linking bottom-up vulnerability analysis with climate projections in the water sector. *Water Resources Research*, 48. doi: <https://doi.org/10.1029/2011WR011212>
- Brunner, L., Lorenz, R., Zumwald, M., & Knutti, R. (2019, 12). Quantifying uncertainty in european climate projections using combined performance-independence weighting. *Environmental Research Letters*, 14. doi: 10.1088/1748-9326/ab492f
- Brunner, L., Pendergrass, A. G., Lehner, F., Merrifield, A. L., Lorenz, R., & Knutti, R. (2020, 11). Reduced global warming from CMIP6 projections when weighting models by performance and independence. *Earth System Dynamic*, 11, 995–1012. doi: <https://doi.org/10.5194/esd-11-995-2020>
- Buchhorn, M., Lesiv, M., Tsendbazar, N.-E., Herold, M., Bertels, L., & Smets, B. (2020). Copernicus Global Land Cover Layers—Collection 2. *Remote Sensing*, 12(6). doi: <https://doi.org/10.3390/rs12061044>
- Bunn, S., & Arthington, A. (2002, 11). Basic principles and ecological consequences of altered flow regimes for aquatic deflation basin lakes. *Environmental management*, 30, 492-507. doi: 10.1007/s00267-002-2737-0
- Chokkavarapu, N., & Mandla, V. R. (2019). Comparative study of GCMs, RCMs, downscaling and hydrological models: a review toward future climate change impact estimation. *Springer Nature Applied Sciences*. doi: <https://doi.org/10.1007/s42452-019-1764-x>
- Conallin, J., Campbell, J., & Baumgartner, L. (2018). Using Strategic Adaptive Management to Facilitate Implementation of Environmental Flow Programs in Complex Social-Ecological Systems. *Environmental Management*, 62, 955-967. doi: 10.1007/s00267-018-1091-9
- Conway, D., Nicholls, R. J., Brown, S., Tebboth, M. G. L., Adger, W. N., Ahmad, B., ... Wester, P. (2019). The need for bottom-up assessments of climate risks and adaptation in climate-sensitive regions. *Nature Climate Change*. doi: <https://doi.org/10.1038/s41558-019-0502-0>

- Culley, S., Noble, S., Yates, A., Timbs, M., Westra, S., Maier, H. R., ... Castelletti, A. (2016). A bottom-up approach to identifying the maximum operational adaptive capacity of water resource systems to a changing climate. *Water Resources Research*, 52, 6751–6768. doi: <https://doi.org/10.1002/2015WR018253>
- de Klerk, A., Oberholster, P., van Wyk, J., de Klerk, L., & Botha, A. (2016). A Watershed Approach in Identifying Key Abiotic Ecosystem Drivers in Support of River Management: a Unique Case Study. *Water Air Soil Pollutino*, 227(196). doi: 10.1007/s11270-016-2864-5
- Deltares. (2022). *Deltares/weathergenr*. Retrieved from <https://github.com/Deltares/weathergenr>
- Department of Water and Sanitation. (2017). *Government Gazette Staatskoerant Part 1 of 2* (Tech. Rep.). Pretoria: Government of South Africa.
- Dwarakish, G., & Ganasri, B. (2015). Impact of land use change on hydrological systems: A review of current modeling approaches. *Cogent Geoscience*, 1(1), 1115691. doi: 10.1080/23312041.2015.1115691
- Engida, T. G., Nigussie, T. A., Aneseyee, A. B., & Barnabas, J. (2021). Land Use/Land Cover Change Impact on Hydrological Process in the Upper Baro Basin, Ethiopia. *Applied and Environmental Soil Science*, 2021. doi: <https://doi.org/10.1155/2021/6617541>
- ESMValTool. (2022). *Climate model weighting by independence and performance (climwip)*. ESM-ValTool Development Team Revision. Retrieved from https://docs.esmvaltool.org/en/latest/recipes/recipe_climwip.html
- Fick, S. E., & Hijmans, R. J. (2017). Worldclim 2: new 1-km spatial resolution climate surfaces for global land areas. *International Journal of Climatology*, 37(12), 4302–4315. doi: <https://doi.org/10.1002/joc.5086>
- Government of South Africa. (2015, December). *The development of the Limpopo Water Management Area North Reconciliation Strategy - Hydrological Analysis* (Strategic Report). Pretoria, South Africa: Department of Water and Sanitation, South Africa.
- World Climate Research Programme's Working Group on Coupled Modelling. (n.d.).
- Fowler, H. J., Blenkinsop, S., & Tebaldi, C. (2007). Linking climate change modelling to impacts studies: recent advances in downscaling techniques for hydrological modelling. *International Journal of Climatology*, 27, 1547–1578. doi: <https://doi.org/10.1002/joc.1556>
- Funk, C., Peterson, P., Landsfeld, M., Pedreros, D., Verdin, J., Shukla, S., ... Michaelsen, J. (2015). The climate hazards infrared precipitation with stations—a new environmental record for monitoring extremes. *Scientific Data*, 2(150066), 6751–6768. doi: <https://doi.org/10.1038/sdata.2015.66>
- Gao, Y., Chen, J., Luo, H., & Wang, H. (2020). Prediction of hydrological responses to land use change. *Science of The Total Environment*, 708. doi: <https://doi.org/10.1016/j.scitotenv.2019.134998>
- García, L., Matthews, J., Rodriguez, D., Wijnen, M., DiFrancesco, K., & Ray, P. (2014). *Beyond Downscaling: A Bottom-up Approach to Climate Adaptation for Water Resources Management* (Guidebook). Washington DC: The World Bank.
- Gosling, S., Taylor, R., Arnell, N., & Todd, M. (2011). A comparative analysis of projected impacts of climate change on river runoff from global and catchment-scale hydrological models. *Hydrology and Earth System Sciences*, 15, 279–294. doi: <https://doi.org/10.5194/hess-15-279-2011>
- Government of South Africa. (2015, March). *The South African Strategy for the Biosphere Programme (2016-2020)* (Strategic Report). Pretoria, South Africa: Department of Environmental Affairs.
- The Global Runoff Data Centre. (2020). *River Discharge*. Retrieved from <https://portal.grdc.bafg.de/> (data retrieved from the GRDC Data Portal)

- Haasnoot, M., Kwakkel, J. H., Walker, W. E., & ter Maat, J. (2013). Dynamic adaptive policy pathways: A method for crafting robust decisions for a deeply uncertain world. *Global Environmental Change*, 23, 485–498. doi: <https://doi.org/10.1016/j.gloenvcha.2012.12.006>
- Hargreaves, G., & Samani, Z. (1985). Reference crop evapotranspiration from temperature. *Applied Engineering in Agriculture*, 1(2), 96-99. doi: <https://doi.org/10.13031/2013.26773>
- Her, Y., Yoo, S., & Cho, J. (2019). Uncertainty in hydrological analysis of climate change: multi-parameter vs. multi-GCM ensemble predictions. *Scientific Reports*, 9(1). doi: <https://doi-org.tudelft.idm.oclc.org/10.1038/s41598-019-41334-7>
- Herman, J. D., Quinn, J. D., Steinschneider, S., Giulliani, M., & Fletcher, S. (2020). Climate Adaptation as a Control Problem: Review and Perspectives on Dynamic Water Resources Planning Under Uncertainty. *Water Resources Research*, 56. doi: <https://doi.org/10.1029/2019WR025502>
- Hersbach, H., Bell, B., Berrisford, P., Hirahara, S., Horányi, A., Muñoz-Sabater, J., ... Thépaut, J.-N. (2020). The ERA5 global reanalysis. *Quarterly Journal of the Royal Meteorological Society*, 146(730), 1999-2049. doi: <https://doi.org/10.1002/qj.3803>
- Imhoff, R., van Verseveld, W., van Osnabrugge, B., & Weerts, A. (2020). Scaling Point-Scale (Pedo)transfer Functions to Seamless Large-Domain Parameter Estimates for High-Resolution Distributed Hydrologic Modeling: An Example for the Rhine River. *Water Resources Research*, 56(4). doi: <https://doi.org/10.1029/2019WR026807>
- Kendall, M. G. (1975). *Rank Correlation Methods*. New York, NY: Oxford University Press.
- Kiesel, J., Stanzel, P., Kling, H., Fohrer, N., Jahrig, S., & Pechlivanidis, I. (2020). Streamflow-based evaluation of climate model sub-selection methods. *Climatic Change*, 163, 1267–1285. doi: <https://doi.org/10.1007/s10584-020-02854-8>
- Kim, D., Chun, J. A., & Choi, S. (2018). Assessing water supply capacity in a complex river basin under climate change using the logistic eco-engineering decision scaling framework. *Hydrology and Earth System Sciences*. doi: <https://doi.org/10.5194/hess-2018-221>
- Knutti, R., Sedláček, J., Sanderson, B., Lorenz, R., Fischer, E., & Eyring, V. (2017). A climate model projection weighting scheme accounting for performance and interdependence. *Geophysical Research Letters*. doi: <https://doi.org/10.1002/2016GL072012>
- Koch, H., Silva, A. L. C., Liersch, S., de Azevedo, J. R. G., & Hattermann, F. F. (2020). Effects of model calibration on hydrological and water resources management simulations under climate change in a semi-arid watershed. *Climatic Change*, 163(3). doi: 10.1007/s10584-020-02917-w
- Kundzewicz, Z., Krysanova, V., Benestad, R., Hov, O., Piniewski, M., & Otto, I. (2018). Uncertainty in climate change impacts on water resources. *Environmental Science & Policy*, 79, 1-8. doi: <https://doi.org/10.1016/j.envsci.2017.10.008>
- Kwakkel, J., & Haasnoot, M. (2019). Supporting DMDU: A Taxonomy of Approaches and Tools. In *Decision Making under Deep Uncertainty* (pp. 355–374). Springer International Publishing. doi: 10.007/978-3-030-05252-2_15
- Lan, T., Lin, K., Xu, C.-Y., Tan, X., & Chen, X. (2020). Dynamics of hydrological-model parameters: mechanisms, problems and solutions. *Hydrology and Earth System Sciences*, 24(3), 1347–1366. doi: 10.5194/hess-24-1347-2020
- Lempert, R. J., Popper, S. W., & Bankes, S. C. (2003). *Shaping the next one hundred years: New methods for quantitative, long-term policy analysis*. Santa Monica, CA: RAND Corporation. doi: <https://doi.org/10.7249/MR1626>
- Li, M., Liang, X., Xiao, C., Zhang, X., Li, G., Li, H., & Jang, W. (2020). Evaluation of Reservoir-Induced Hydrological Alterations and Ecological Flow Based on Multi-Indicators. *Water*, 12(2069). doi: <https://doi.org/10.3390/w12072069>

- Liu, Y., Zhang, J., Yang, Q., Zhou, X., & Wang, G. (2021). Changes in and modelling of hydrological process for a semi-arid catchment in the context of human disturbance. *Frontiers in Earth Science*, 9. doi: 10.3389/feart.2021.759534
- Lorenz, R., Herger, N., Sedlacek, J., Eyring, V., Fischer, E. M., & Knutti, R. (2018). Prospects and Caveats of Weighting Climate Models for Summer Maximum Temperature Projections Over North America. *Journal of Geophysical Research: Atmospheres*. doi: <https://doi-org.tudelft.idm.oclc.org/10.1029/2017JD027992>
- Lyon, A., Hunter-Jones, P., & Warnaby, G. (2017). Are we any closer to sustainable development? Listening to active stakeholder discourses of tourism development in the Waterberg Biosphere Reserve, South Africa. *Tourism Management*, 61, 234–247. doi: <http://dx.doi.org/10.1016/j.tourman.2017.01.010>
- Maeko, M. (2020). *An evaluation of the ecological impacts of sand mining on the Mokolo River in Lephale, South Africa* (Unpublished doctoral dissertation). University of South Africa.
- Mann, H. B. (1945). Nonparametric tests against trend. *Econometrica*, 13, 245–259. doi: <https://doi.org/10.2307/1907187>
- Masson-Delmotte, V., Zhai, P., Pirani, A., Connors, S. L., Péan, S., C. Berger, Caud, N., ... (eds.), Z. B. (2021). *Climate Change 2021: The Physical Science Basis. Contribution of Working Group I to the Sixth Assessment Report of the Intergovernmental Panel on Climate Change* (Scientific Report). Cambridge University Press: IPCC.
- Mendoza, G., Jeuken, A., Matthews, J. H., Stakhiv, E., Kucharski, J., & Gilroy, K. (2018). *Climate Risk Informed Decision Analysis (CRIDA). Collaborative Water Resources Planning for an Uncertain Future* (Guidebook). Paris, France: UNESCO.
- Mengistu, A. G., van Rensburg, L. D., & Woyessa, Y. E. (2019). Techniques for calibration and validation of SWAT model in data scarce arid and semi-arid catchments in South Africa. *Journal of Hydrology: Regional Studies*, 25(100621). doi: 10.1016/j.ejrh.2019.100621.
- Merrifield, A. L., Brunner, L., Lorenz, R., Medhaug, I., & Knutti, R. (2020). An investigation of weighting schemes suitable for incorporating large ensembles into multi-model ensembles. *Earth System Dynamics*, 11, 807–834. doi: <https://doi.org/10.5194/esd-11-807-2020>
- Mulligan, M., van Soesbergen, A., & Sáenz, L. (2020). GOODD, a global dataset of more than 38,000 georeferenced dams. *Science Data*, 7(31). doi: <https://doi.org/10.1038/s41597-020-0362-5>
- Murphy, J. (1998). An Evaluation of Statistical and Dynamical Techniques for Downscaling Local climate. *Journal of Climate*, 12, 2256–2284. doi: [https://doi.org/10.1175/1520-0442\(1999\)12<2256:AEOSTD>2.0.CO;2](https://doi.org/10.1175/1520-0442(1999)12<2256:AEOSTD>2.0.CO;2)
- Nash, J., & Sutcliffe, J. (1970). River flow forecasting through conceptual models part I — A discussion of principles. *Journal of Hydrology*, 10(3), 282-290. doi: [https://doi.org/10.1016/0022-1694\(70\)90255-6](https://doi.org/10.1016/0022-1694(70)90255-6)
- Nijzink, R., Hutton, C., Pechlivanidis, I., Capell, R., Arheimer, B., Freer, J., ... Hrachowitz, M. (2016). The evolution of root-zone moisture capacities after deforestation: a step towards hydrological predictions under change? *Hydrology and Earth System Sciences*, 20(12), 4775–4799. doi: 10.5194/hess-20-4775-2016
- National Oceanic and Atmospheric Administration. (2020). *Past Weather Rainfall Limpopo*. Retrieved from <https://www.ncei.noaa.gov/access/past-weather/> (data retrieved from the NOAA Data Portal)
- Olden, J. D., & Poff, N. L. (2003). Redundancy and the Choice of Hydrologic Indices for Characterizing Streamflow Regimes. *River Research and Applications*, 19, 101-121. doi: <https://doi.org/10.1002/rra.700>
- Pahl-Wostl, C., Arthington, A., Bogardi, J., Bunn, S., Hoff, H., Lebel, L., ... Tsegai, D. (2013). Environmental flows and water governance: managing sustainable water uses. *Current Opinion in Environmental Sustainability*, 5, 341–351. doi: <http://dx.doi.org/10.1016/j.cosust.2013.06.009>

- Pastén-Zapata, E., Pimentel, R., Royer-Gaspard, P., Sonnenborg, T. O., Aparicio-Ibañez, J., Lemoine, A., ... Refsgaard, J. C. (2022). The effect of weighting hydrological projections based on the robustness of hydrological models under a changing climate. *Journal of Hydrology: Regional Studies*, *41*, 101113. doi: <https://doi.org/10.1016/j.ejrh.2022.101113>
- Penas, F. J., Barquin, J., & Álvarez, C. (2016). Assessing hydrologic alteration: Evaluation of different alternatives according to data availability. *Ecological Indicators*, *60*, 470-482. doi: <https://doi.org/10.1016/j.ecolind.2015.07.021>
- Poff, N. (2018). Beyond the natural flow regime? Broadening the hydro-ecological foundation to meet environmental flows challenges in a non-stationary world. *Freshwater Biology*, *63*, 1011–1021. doi: <https://doi.org/10.1111/fwb.13038>
- Poff, N., Allan, J., Palmer, M., Hart, D., Richter, B., Arthington, A., ... Stanford, J. (2003). River Flows and Water Wars: Emerging Science for Environmental Decision Making. *Frontiers in Ecology and the Environment*, *1*(6), 298-306. doi: [10.2307/3868090](https://doi.org/10.2307/3868090)
- Poff, N., Brown, C. E., G. T., Matthews, J. H. A., P. M., Spence, C. M., ... A., B. (2015). Sustainable water management under future uncertainty with eco-engineering decision scaling. *Nature Climate Change*, *6*(2016), 25–34. doi: <https://doi.org/10.1038/NCLIMATE2765>
- Poff, N., & Matthews, J. (2013). Environmental flows in the Anthropocene: past progress and future prospects. *Current Opinion in Environmental Sustainability*, *5*(2016), 667–675. doi: <http://dx.doi.org/10.1016/j.cosust.2013.11.006>
- Poff, N., & Zimmerman, J. (2010). Ecological responses to altered flow regimes: a literature review to inform the science and management of environmental flows. *Freshwater Biology*, *55*, 194-205. doi: [10.1111/j.1365-2427.2009.02272.x](https://doi.org/10.1111/j.1365-2427.2009.02272.x)
- Poggio, L., de Sousa, L. M., Batjes, N. H., Heuvelink, G. B. M., Kempen, B., Ribeiro, E., & Rossiter, D. (2021). SoilGrids 2.0: producing soil information for the globe with quantified spatial uncertainty. *Soil*, *7*, 217-240. doi: <https://doi.org/10.5194/soil-7-217-2021>
- Prucha, B., Graham, D., Watson, M., Avenant, M., Esterhuyse, S., Joubert, A., ... Vos, T. (2016). MIKE-SHE integrated groundwater and surface water model used to simulate scenario hydrology for input to DRIFT-ARID: the Mokolo River case study. *Water SA*, *42*(3), 384–398. doi: <http://dx.doi.org/10.4314/wsa.v42i3.03>
- Qureshi, S., Koohpayma, J., Firozjaei, M. K., & Kakroodi, A. A. (2022). Evaluation of Seasonal, Drought, and Wet Condition Effects on Performance of Satellite-Based Precipitation Data over Different Climatic Conditions in Iran. *Remote Sensing*, *14*(1). doi: [10.3390/rs14010076](https://doi.org/10.3390/rs14010076)
- Ray, P., Wi, S., Schwarz, A., Correa, M., He, M., & Brown, C. (2020). Vulnerability and risk: climate change and water supply from California's Central Valley water system. *Climate Change*, *161*, 177–199. doi: <https://doi.org/10.1007/s10584-020-02655-z>
- Richter, B., van Baumgartner, J., Powell, J., & Braun, D. (1996). A Method for Assessing Hydrologic Alteration within Ecosystems. *Conservation Biology*, *10*(4), 1163–1174. doi: <http://www.jstor.org/stable/2387152>
- River Health Programme. (2006). *State-of-Rivers Report: the Mokolo River System* (Tech. Rep.). Pretoria: Department of Environmental Affairs and Tourism.
- Rocheta, E., Sugiyanto, M., Johnson, F., Evans, J., & A., S. (2014). How well do general circulation models represent low-frequency rainfall variability? *Water Resources Research*, *50*, 2108-2123. doi: <https://doi.org/10.1002/2012WR013085>
- Samaniego, L., Kumar, R., & Attinger, S. (2010). Multiscale parameter regionalization of a grid-based hydrologic model at the mesoscale. *Water Resources Research*, *46*(5). doi: <https://doi.org/10.1029/2008WR007327>

- Schellekens, J., van Verseveld, W., Visser, M., Winsemius, H., Euser, T., Bouaziz, L., ... Benedict, I. (2021). *openstreams/wflow: unstable-master*. Deltares. Retrieved from <https://github.com/openstreams/wflow>
- Seaman, M., Watson, M., Avenant, M., Joubert, A., King, J., Barker, C., ... Vos, T. (2016). DRIFT-ARID: Application of a method for environmental water requirements (EWRs) in a non-perennial river (Mokolo River) in South Africa. *Water South Africa*, 42(3). doi: <http://dx.doi.org/10.4314/wsa.v42i3.02>
- Shortridge, J. E., & Guikema, S. D. (2016). Scenario Discovery with Multiple Criteria: An Evaluation of the Robust Decision-Making Framework for Climate Change Adaptation. *Risk Analysis*, 36(12), 2298–2312. doi: [10.1111/risa.12582](https://doi.org/10.1111/risa.12582)
- Sperna Weiland, F. C., Visser, R. D., Greve, P., Bisselink, B., Brunner, L., & Weerts, A. H. (2021). Estimating regionalized hydrological impacts of climate change over Europe by performance-based weighting of CORDEX projections. *Frontiers in Water*, 3. doi: [10.3389/frwa.2021.713537](https://doi.org/10.3389/frwa.2021.713537)
- Stainforth, D., Downing, T. E., Washington, R., Lopez, A., & New, M. (2007). Issues in the interpretation of climate model ensembles to inform decisions. *Philosophical Transactions of the Royal Society A: Mathematical, Physical and Engineering Sciences*, 365(1857), 2163–2177. doi: <https://doi.org/10.1098/rsta.2007.2073>
- Steinschneider, S., & Brown, C. (2013). A semiparametric multivariate, multisite weather generator with low-frequency variability for use in climate risk assessments. *Water Resources Research*, 49, 7205–7220. doi: <https://doi.org/10.1002/wrcr.20528>
- Steinschneider, S., Herman, J., Kucharski, J., Abellera, M., & Ruggiero, P. (2022). Uncertainty decomposition to understand the influence of water systems model error in climate vulnerability assessments. *ESSOar*, 42. doi: <https://doi.org/10.1002/essoar.10510888.1>
- Steinschneider, S., McCrary, R., Mearns, L., & Brown, C. (2015). The effects of climate model similarity on probabilistic climate projections and the implications for local, risk-based adaptation planning. *Geophysical Research Letters*, 42, 5014–5022. doi: [10.1002/2015GL064529](https://doi.org/10.1002/2015GL064529)
- The Nature Conservancy. (2019). *Environmental flows*. Conservation Gateway. Retrieved from <https://www.conservationgateway.org/ConservationPractices/Freshwater/EnvironmentalFlows/Pages/environmental-flows.aspx>
- van den Hurk, B., Siegmund, P., & Klein Tank, A. (2014). *KNMI'14: Climate Change scenarios for the 21st Century – A Netherlands perspective* (<https://doi.org/scientific-report>). De Bilt, the Netherlands: KNMI.
- Verbist, K. M. J., Maureira-Cortés, H., Rojas, P., & Vicuna, S. (2020). A stress test for climate change impacts on water security: A CRIDA case study. *Climate Risk Management*, 28(100222). doi: [10.1016/j.crm.2020.100222](https://doi.org/10.1016/j.crm.2020.100222)
- Videira, N., Antunes, P., Santos, R., & Gamito, S. (2003). Participatory Modelling in Environmental Decision-Making: The Ria Formosa Natural Park Case Study. *Journal of Environmental Assessment Policy and Management*, 5(3). doi: <https://doi.org/10.1142/S1464333203001371>
- Weerts, A., Van Verseveld, W., Eilander, D., Boisgontier, H., Haag, H., Hazenberg, P., & Imhoff, R. (2020). *Testing the distributed hydrological wflow-sbm concept across different geographical domains*. Retrieved from https://presentations.copernicus.org/EGU2020/EGU2020-10886_presentation.pdf (EGU conference presentation slides)
- Whateley, S., Steinschneider, S., & Brown, C. (2016). Selecting Stochastic Climate Realizations to Efficiently Explore a Wide Range of Climate Risk to Water Resource Systems. *Water Resources Planning and Management*. doi: [https://doi.org/10.1061/\(ASCE\)WR.1943-5452.0000631](https://doi.org/10.1061/(ASCE)WR.1943-5452.0000631)

- Xiong, M., Liu, P., Cheng, L., Deng, C., Gui, Z., Zhang, X., & Liu, Y. (2017). Identifying time-varying hydrological model parameters to improve simulation efficiency by the ensemble kalman filter: A joint assimilation of streamflow and actual evapotranspiration. *Journal of Hydrology*, 568(12), 758-768. doi: <https://doi.org/10.1016/j.jhydrol.2018.11.038>
- Öztürk, M., Coptý, N. K., & Saysel, A. K. (2013). Modeling the impact of land use change on the hydrology of a rural watershed. *Journal of Hydrology*, 497, 97-109. doi: <https://doi.org/10.1016/j.jhydrol.2013.05.022>

A | Hydrological Model

A hydrological model was developed for the Mokolo River with a wflow-sbm model. The hydrographs in Figure A.1 and A.2 present the modelled and observed total annual and average monthly discharge respectively at the four gauge stations. Tables A.1 and A.2 show the performance of the calibrated wflow-sbm model during the dry and wet season respectively.

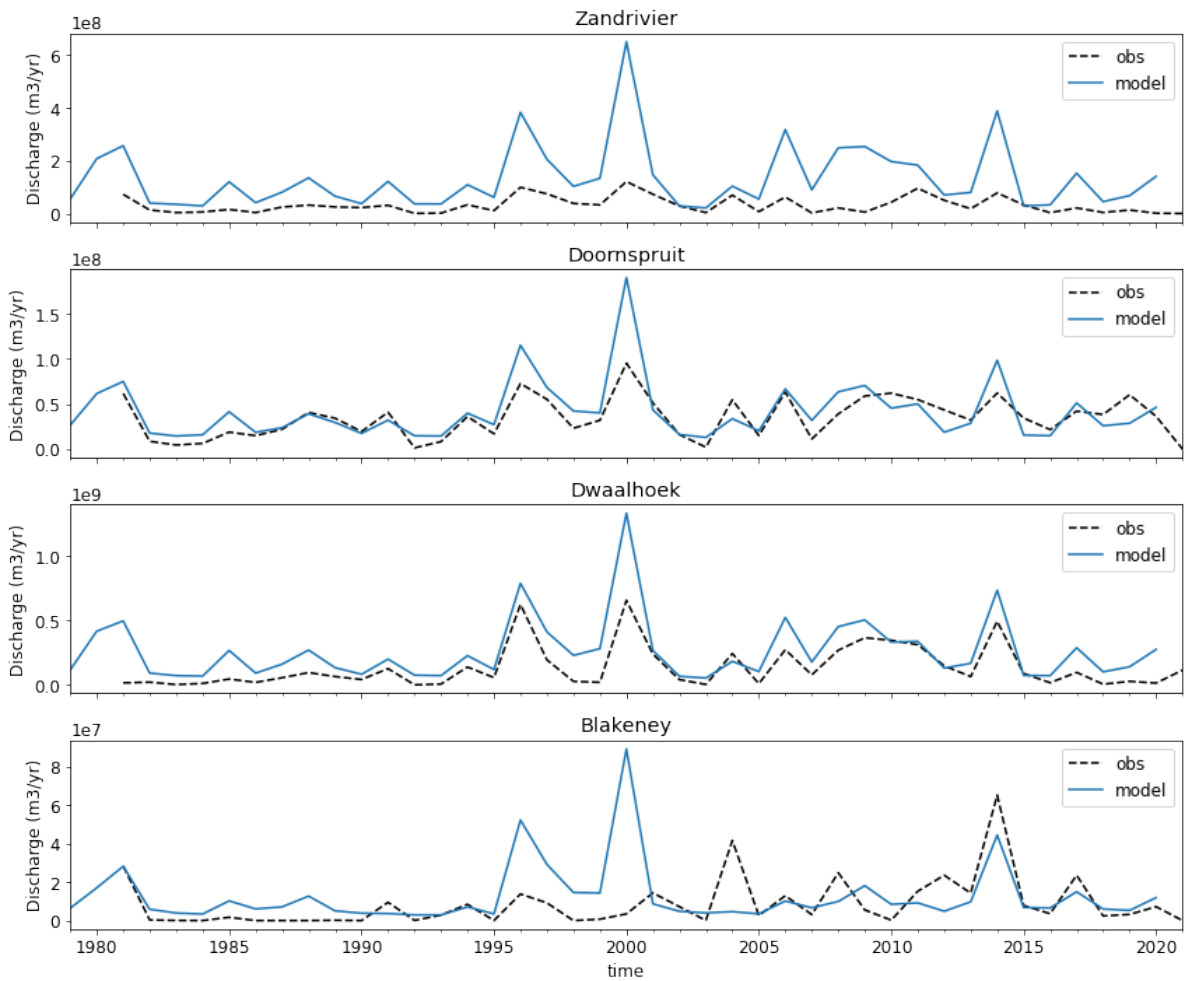


Figure A.1 – Total annual discharge in m3/yr for the four locations with observation stations. Note the different vertical axes.

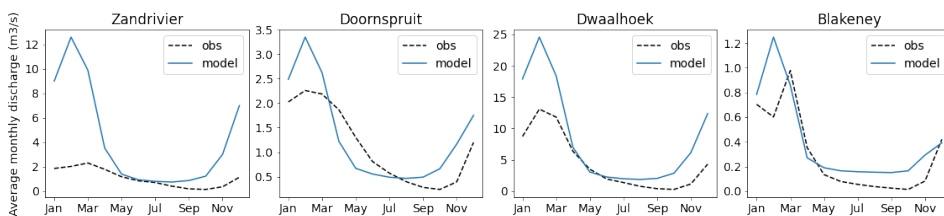


Figure A.2 – Modelled and observed average monthly discharge in m3/s at the four gauge stations. Note the different vertical axes.

Table A.1 – Model performance compared to observed flows during the dry season (April-October). Except for the Nash Sutcliffe Efficiencies (first two columns), the metrics are computed as root-mean-square errors. Daily mean refers to mean error of all daily flows between 1981-2020.

	NS (-)	NSlog (-)	Daily mean (m³/s)	Annual mean (m³/s)	BFI (-)	Low pulse count (-)	High pulse count (-)	Low pulse duration (d)
Doornspruit	-1.2	0.8	-0.1	0.4	0.7	42.4	36.0	44.2
Dwaalhoek	-2.6	-0.5	3.3	1.7	1.1	35.9	25.9	71.1
Zandrivier	-4.1	-0.4	1.7	0.9	1.0	45.1	25.8	65.4
Blakeney	-1.2	-0.9	0.2	0.1	1.4	87.9	51.4	80.0

Table A.2 – Model performance compared to observed flows during the wet season (November to March). Except for the Nash Sutcliffe Efficiencies (first two columns), the metrics are computed as root-mean-square errors. Daily mean refers to mean error of all daily flows between 1981-2020.

	NS (-)	NSlog (-)	Daily mean (m³/s)	Annual mean (m³/s)	BFI (-)	Low pulse count (-)	High pulse count (-)	Low pulse duration (d)
Doornspruit	-13.5	0.2	6.6	1.2	0.6	33.8	25.7	18.5
Dwaalhoek	-1.9	0.2	37.1	8.7	0.5	39.1	32.2	37.7
Zandrivier	-119.3	-0.3	24.5	7.7	0.8	46.2	34.3	21.6
Blakeney	-0.7	0.2	2.7	0.9	0.8	100.1	54.1	47.9

B | ERA5 precipitation scaling

ERA5 monthly precipitation was bias corrected to spatially averaged observed rainfall between 1980 and 1997, using the empirical quantile mapping technique of Amengual et al. (2012). Figures B.1, B.2 and B.3 present the spatially averaged rainfall sum and distributions of the original ERA5 data, the scaled ERA5 data and the observations during the period that was used for correction.

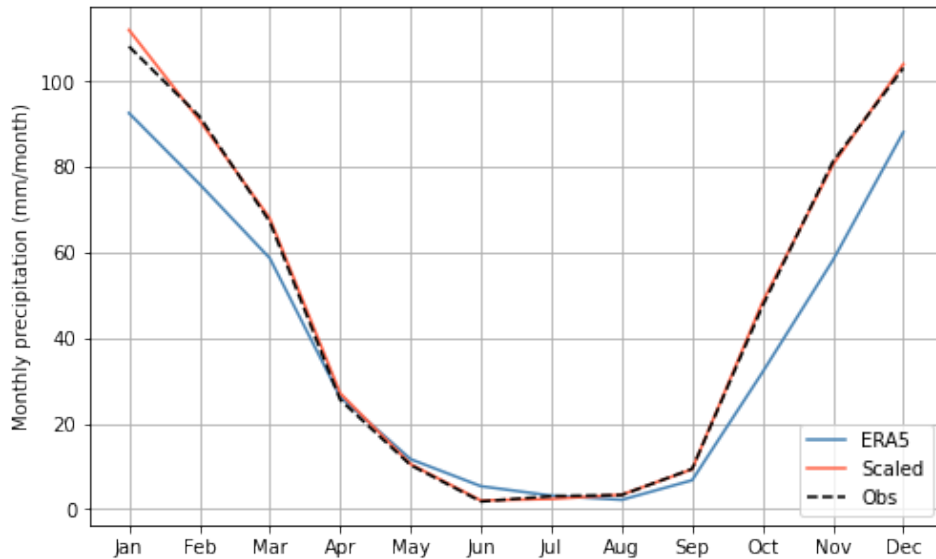


Figure B.1 – Total average monthly precipitation between 1980-1997 for ERA5, observed, and bias corrected ERA5 data.

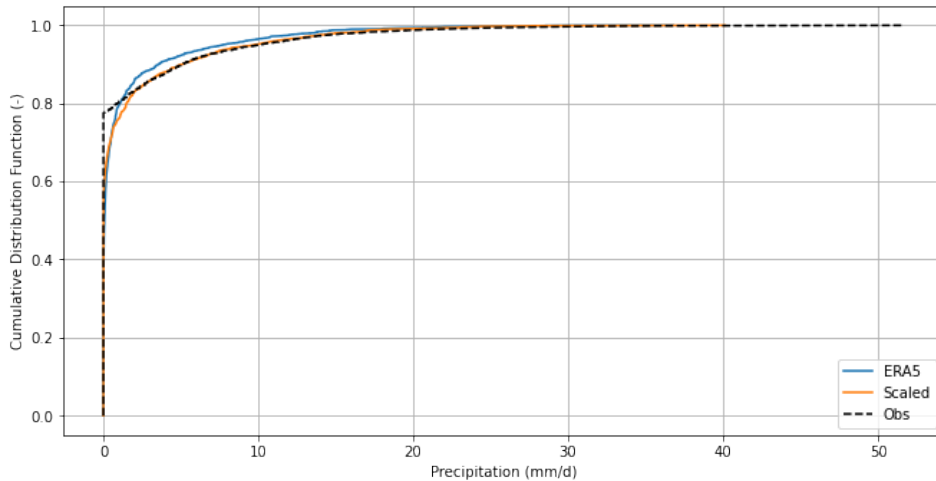


Figure B.2 – Cumulative distribution function for ERA5, observed, and bias corrected ERA5 precipitation data between 1980-1997.

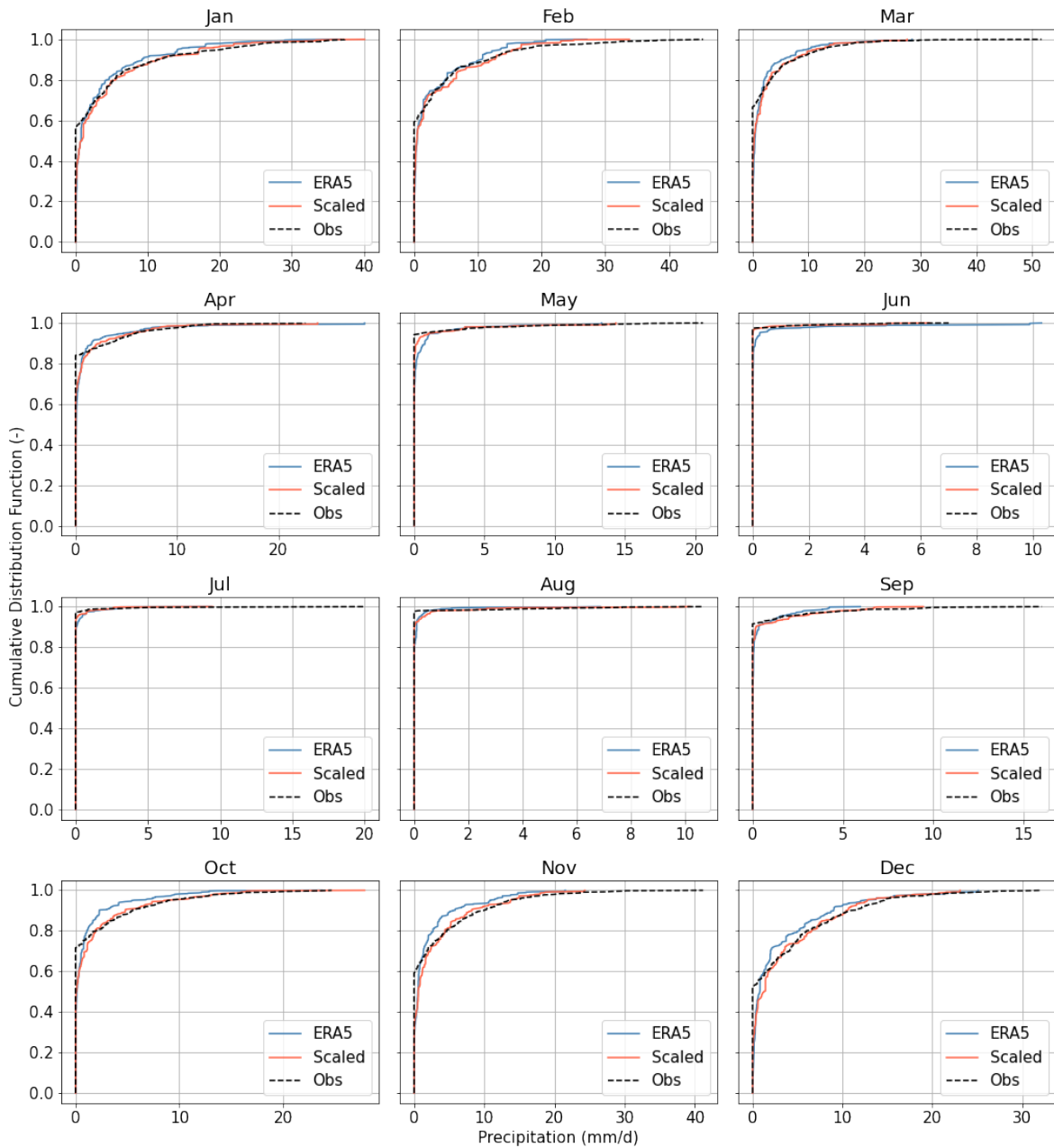


Figure B.3 – Monthly cumulative distribution function for ERA5, observed, and bias corrected ERA5 precipitation data between 1980-1997.

C | Global Climate Models

Monthly precipitation and temperature from 48 different CMIP5 models were collected from this study. An overview of this can be found in Table C.1. The table moreover shows for which emission scenarios (RCPs) the models provide projections for 2020-2080. All models provide historical reanalysis for precipitation and temperature between 1960 and 2005.

Table C.1 – Overview of the CMIP5 Global Climate Models used.

Model name	RCP 2.6	RCP 4.5	RCP 6.0	RCP 8.5
ACCESS1-0		x		x
ACCESS1-3		x		x
bcc-csm1-1	x	x	x	x
bcc-csm1-1-m	x	x	x	x
BNU-ESM	x	x		x
CanCM4		x		
CanESM2	x	x		x
CCSM4	x	x	x	x
CESM1-BGC		x		x
CESM1-CAM5	x	x	x	x
CMCC-CESM				x
CMCC-CM		x		x
CMCC-CMS		x		x
CNRM-CM5	x	x		x
CSIRO-Mk3-6-0	x	x	x	x
EC-EARTH				x
FGOALS-g2	x	x		x
FIO-ESM	x	x	x	x
GFDL-CM2p1		x		
GFDL-CM3	x	x	x	x
GFDL-ESM2G	x	x	x	x
GFDL-ESM2M		x	x	x
GISS-E2-H	x	x	x	x
GISS-E2-H-CC		x		
GISS-E2-R	x	x	x	x
GISS-E2-R-CC		x		
HadCM3		x		
HadGEM2-AO	x	x	x	x
HadGEM2-CC		x		x
HadGEM2-ES	x	x	x	x
inmcm4		x		x
IPSL-CM5A-LR	x	x	x	x
IPSL-CM5A-MR	x	x	x	x
IPSL-CM5B-LR		x		x
IPSL-CM5B-MR		x		x
MIROC4h		x		
MIROC5	x	x	x	x
MIROC-ESM	x	x	x	x
MIROC-ESM-CHEM	x	x	x	x
MPI-ESM-LR	x	x	x	x
MPI-ESM-MR	x	x	x	x
MRI-CGCM3	x	x	x	x
NorESM1-M	x	x	x	x
NorESM1-ME	x	x	x	x
Total	26	41	21	37

D | GCM projections

Boxplots of monthly GCM projections for a relative change in precipitation and temperature can be found in Figures D.1 and D.2 respectively. The boxplots in Figure D.3 show the relative change in precipitation during the wet and dry season.

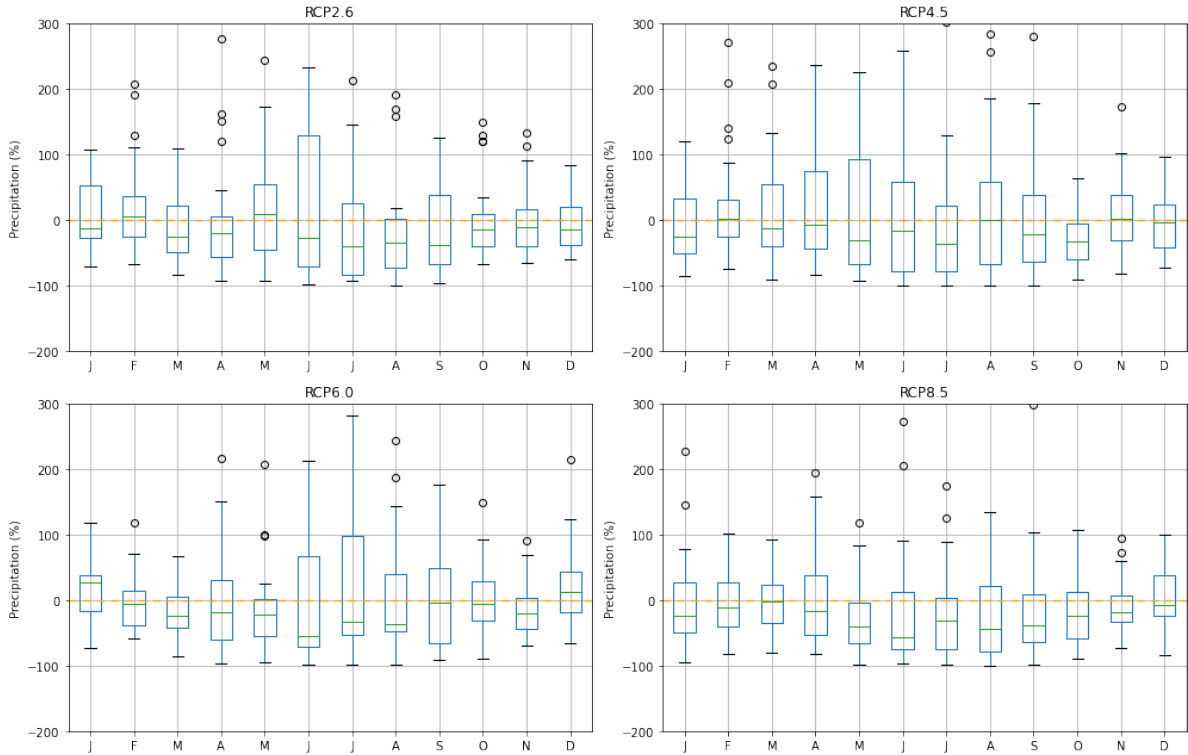


Figure D.1 – Monthly GCM projections of precipitation for 2020-2060 relative to 1980-2005.

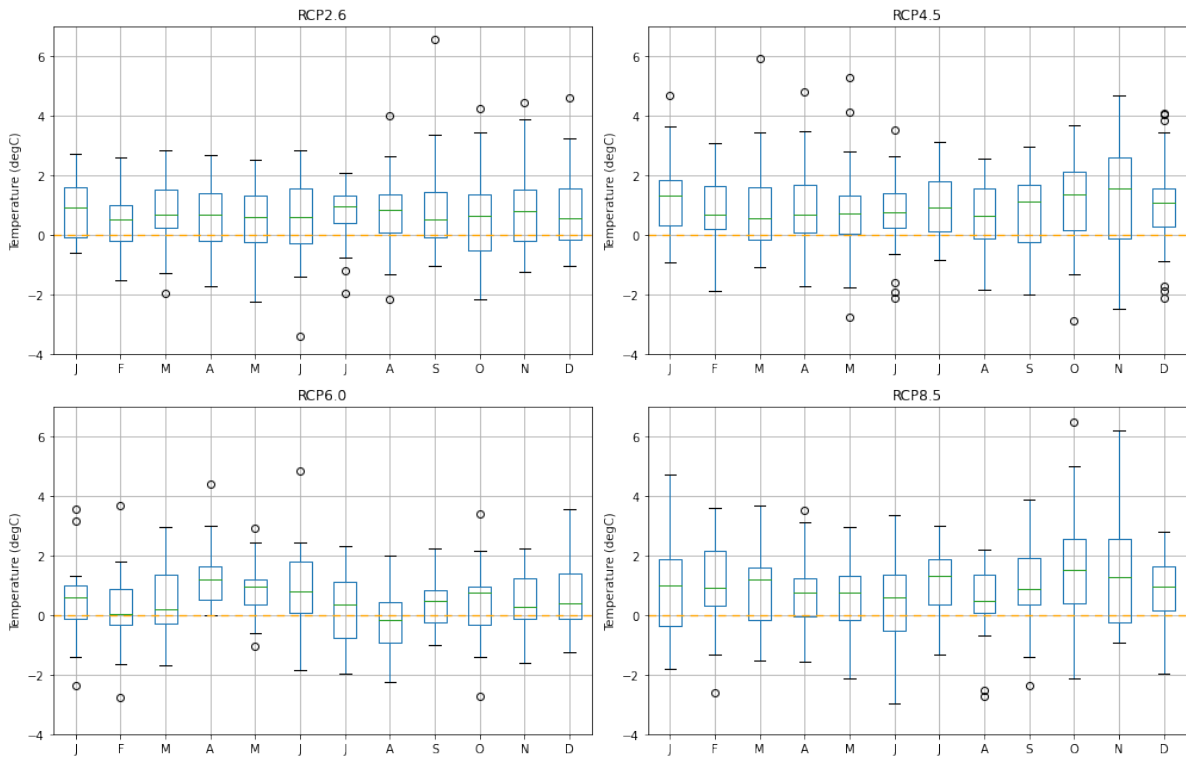


Figure D.2 – Monthly GCM projections of temperature for 2020-2060 relative to 1980-2005.

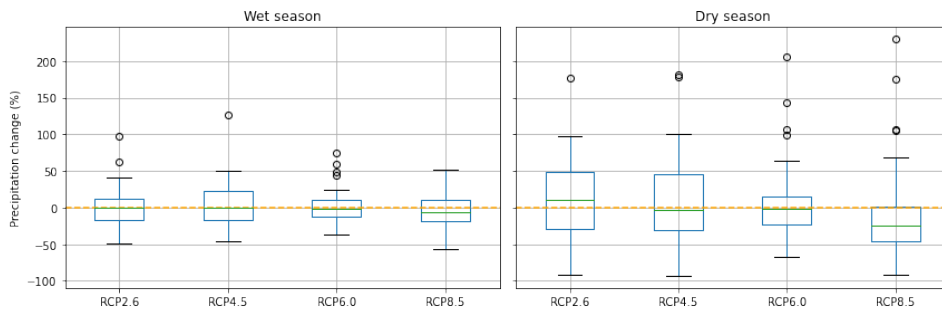


Figure D.3 – Boxplots of relative average seasonal precipitation changes between 1960-2000 and 2020-2060 for the four RCP scenarios in the wet season (October-April) and the dry season (May-September).

E | Climate stress test

Relative changes in the flow indicators to average annual changes in precipitation and temperature are presented in Figure E.1.

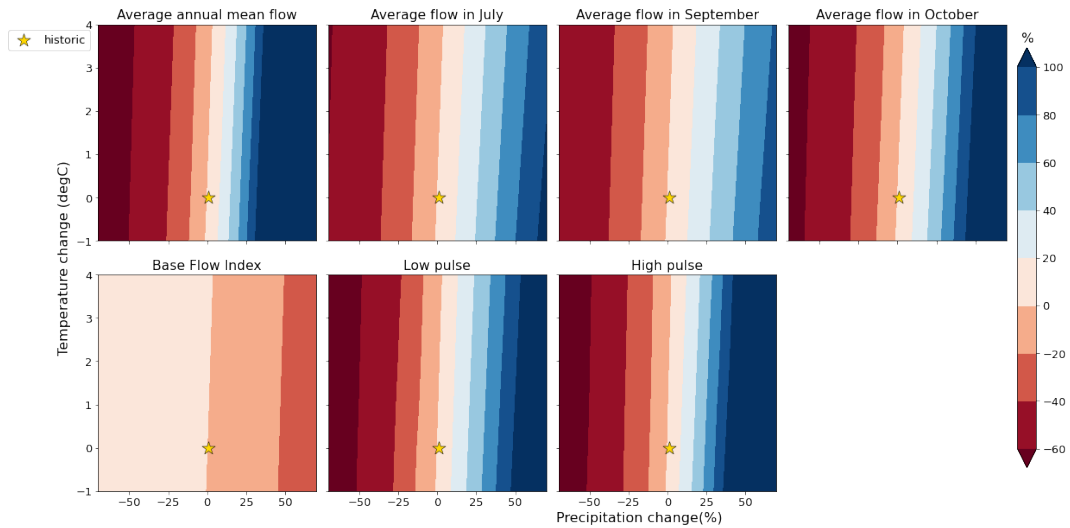


Figure E.1 – Responses to temperature and precipitation changes for seven flow indicators at Dwaalhoek. The flow, temperature and precipitation changes indicate relative changes between historical (1980-2020) and future (2020-2060) conditions. The yellow star indicates the historical river flow and climate conditions.

F | Global Climate Model Weighting

The correlation between historical average annual precipitation (pr_{ANN}), dry season precipitation (pr_{JJA}), and average temperature (tas_{ANN}) in the GCMs is presented in Figure F.1. Furthermore, Figure F.2 shows the influence of the performance and dependence sigmas on the distribution of the weights over the GCMs. It can be seen that the value of the performance sigma has significantly more influence than the dependence sigma. This is also illustrated in Figure F.3.

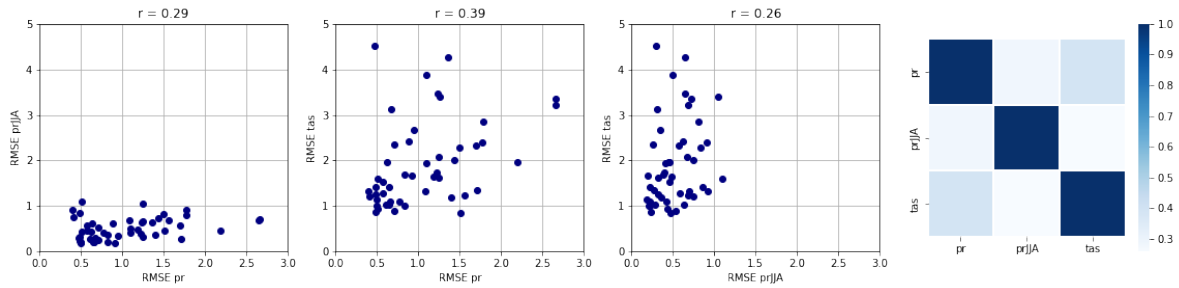


Figure F.1 – Correlation between the three weighting diagnostics and a heat map of the Pearson correlation coefficients (right).

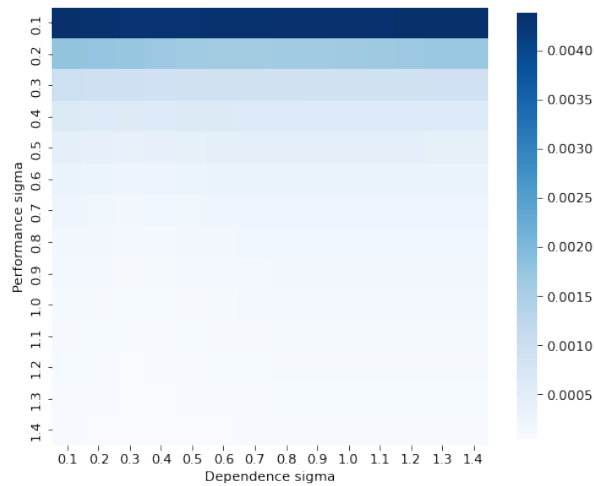


Figure F.2 – Variance of model weights for different combinations of performance and dependence sigma's.

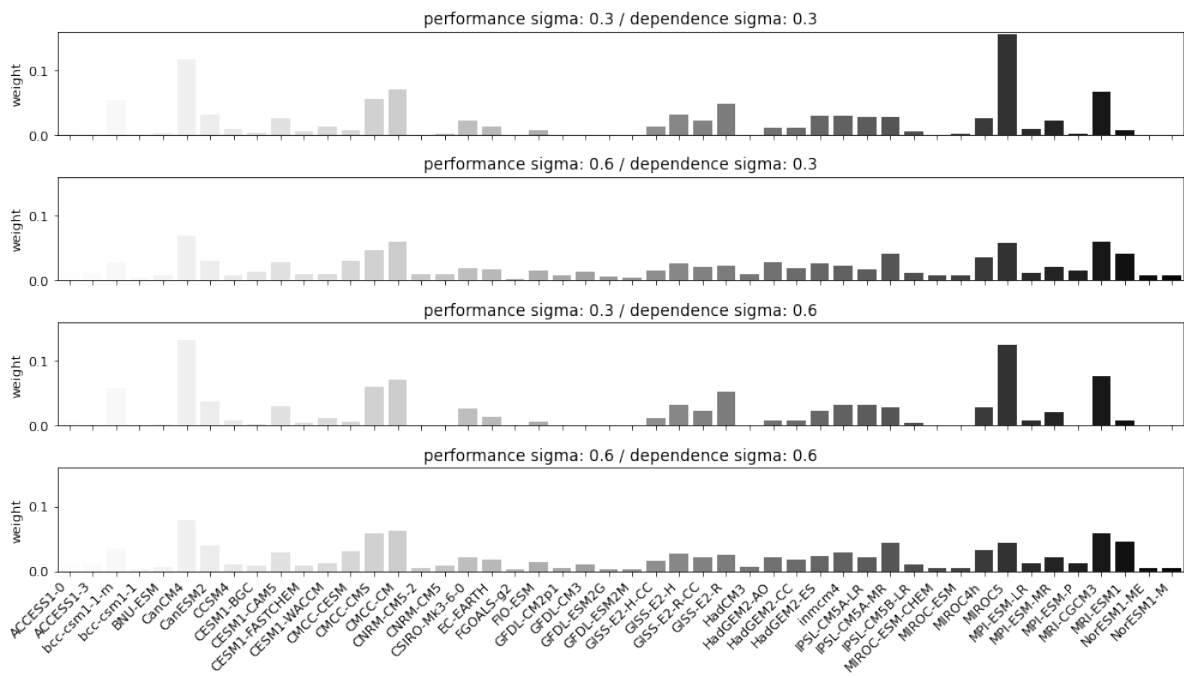


Figure F.3 – Model weights for four combinations of performance and dependence sigma's.